Acta Pharmaceutica Sinica B 2023;13(3):1036−1052

Chinese Pharmaceutical Association
Institute of Materia Medica, Chinese Academy of Medical Sciences

Acta Pharmaceutica Sinica B

www.elsevier.com/locate/apsb
www.sciencedirect.com

ORIGINAL ARTICLE

Compound Danshen Dripping Pill inhibits hypercholesterolemia/atherosclerosis-induced heart failure in ApoE and LDLR dual deficient mice *via* multiple mechanisms

Yanfang Yang[a,†], Ke Feng[b,†], Liying Yuan[a], Yuxin Liu[a], Mengying Zhang[c], Kaimin Guo[c], Zequn Yin[d], Wenjia Wang[c], Shuiping Zhou[e,f], He Sun[c,e,f], Kaijing Yan[c,e,f], Xijun Yan[e,f], Xuerui Wang[d], Yajun Duan[d,g,*], Yunhui Hu[c,*], Jihong Han[a,d,*]

[a]*College of Life Sciences, State Key Laboratory of Medicinal Chemical Biology, Key Laboratory of Bioactive Materials of Ministry of Education, Nankai University, Tianjin 300071, China*
[b]*Department of Physiology, Binzhou Medical University, Yantai 264003, China*
[c]*Cloudphar Pharmaceuticals Co., Ltd., Shenzhen 518000, China*
[d]*Key Laboratory of Metabolism and Regulation for Major Diseases of Anhui Higher Education Institutes, Hefei University of Technology, Hefei 230009, China*
[e]*The State Key Laboratory of Core Technology in Innovative Chinese Medicine, Tasly Academy, Tasly Holding Group Co., Ltd., Tianjin 300410, China*
[f]*Tasly Pharmaceutical Group Co., Ltd., Tianjin 300410, China*
[g]*Department of Cardiology, the First Affiliated Hospital of USTC, Division of Life Science and Medicine, University of Science and Technology of China, Hefei 230001, China*

Received 11 August 2022; received in revised form 19 September 2022; accepted 10 October 2022

KEY WORDS

Compound danshen dripping pill;
Heart failure;
Hypercholesterolemia;

Abstract Heart failure is the leading cause of death worldwide. Compound Danshen Dripping Pill (CDDP) or CDDP combined with simvastatin has been widely used to treat patients with myocardial infarction and other cardiovascular diseases in China. However, the effect of CDDP on hypercholesterolemia/atherosclerosis-induced heart failure is unknown. We constructed a new model of heart failure induced by hypercholesterolemia/atherosclerosis in apolipoprotein E (ApoE) and LDL receptor (LDLR) dual

*Corresponding authors. Tel.: +86 17352916451 (Yajun Duan); +86 18522755110 (Yunhui Hu); +86 13920545670 (Jihong Han).
E-mail addresses: yduan@hfut.edu.cn (Yajun Duan), tsl-huyunhui@tasly.com (Yunhui Hu), jihonghan2008@nankai.edu.cn (Jihong Han).
[†]These authors made equal contributions to this work.
Peer review under responsibility of Chinese Pharmaceutical Association and Institute of Materia Medica, Chinese Academy of Medical Sciences.

https://doi.org/10.1016/j.apsb.2022.11.012
2211-3835 © 2023 Chinese Pharmaceutical Association and Institute of Materia Medica, Chinese Academy of Medical Sciences. Production and hosting by Elsevier B.V. This is an open access article under the CC BY-NC-ND license (http://creativecommons.org/licenses/by-nc-nd/4.0/).

Atherosclerosis;
Simvastatin;
ApoE$^{-/-}$LDLR$^{-/-}$ mice;
Inflammation;
Oxidative stress

deficient (ApoE$^{-/-}$LDLR$^{-/-}$) mice and investigated the effect of CDDP or CDDP plus a low dose of simvastatin on the heart failure. CDDP or CDDP plus a low dose of simvastatin inhibited heart injury by multiple actions including anti-myocardial dysfunction and anti-fibrosis. Mechanistically, both Wnt and lysine-specific demethylase 4A (KDM4A) pathways were significantly activated in mice with heart injury. Conversely, CDDP or CDDP plus a low dose of simvastatin inhibited Wnt pathway by markedly up-regulating expression of Wnt inhibitors. While the anti-inflammation and anti-oxidative stress by CDDP were achieved by inhibiting KDM4A expression and activity. In addition, CDDP attenuated simvastatin-induced myolysis in skeletal muscle. Taken together, our study suggests that CDDP or CDDP plus a low dose of simvastatin can be an effective therapy to reduce hypercholesterolemia/atherosclerosis-induced heart failure.

© 2023 Chinese Pharmaceutical Association and Institute of Materia Medica, Chinese Academy of Medical Sciences. Production and hosting by Elsevier B.V. This is an open access article under the CC BY-NC-ND license (http://creativecommons.org/licenses/by-nc-nd/4.0/).

1. Introduction

Heart failure, caused by a structural and/or functional cardiac abnormality, is the leading cause of death worldwide[1,2]. Many risk factors, such as age, coronary heart disease (CHD), high blood pressure, valvular heart disease, left ventricular hypertrophy, diabetes and obesity, can make contributions to heart failure. With increased prevalence of heart failure, the novel treatment strategies have been constantly created. To date, the medicines for treatment of heart failure patients include diuretics, statins, and blockers for angiotensin receptor, β-receptor and calcium channel. Despite the advances in modern biology and medicine, heart failure still remains as a leading cause of mortality and morbidity, which may be attributed to the limited efficacy and side effects of the medicines[3]. For example, statins have beneficial effects to heart failure. However, the long-term of statin therapy may cause some side-effects including myopathy[4], which can result in statin intolerance in the patients.

Traditional Chinese medicine has been used to treat various diseases with a long history in China. It can also be considered as an effective alternative or complementary therapy for many kinds of diseases. The Compound Danshen Dripping Pill (CDDP, T89, Tasly), a traditional Chinese medicine, has been widely used in prevention and treatment of myocardial ischemia and other cardiovascular diseases in clinic[5]. CDDP contains components extracted from *Saviae miltiorrhizae* Bunge, *Panax notoginseng* Burkill and borneol using the modern medical technology[6]. Many studies have reported that CDDP and/or its components have protective effects on myocardial injury by inhibiting inflammation, oxidative stress and fibrosis[5]. Indeed, CDDP or CDDP combined simvastatin has been used to reduce CHD in patients. However, whether CDDP alone or combined simvastatin can protect against heart failure remains unclarified.

Wnt signaling is a highly conserved pathway in biological evolution, and plays key roles in many biological processes[7]. Typically, it includes canonical and noncanonical pathways. The canonical Wnt pathway is mediated through β-catenin, whereas the non-canonical Wnt pathway by planner cell polarity and Ca^{2+} pathways[7]. In addition, both canonical and noncanonical Wnt pathways can be influenced by some endogenous inhibitors, such as Wnt inhibitory factor (WIF), Dickkopfs (DKKs), and secreted frizzled-related proteins (SFRPs)[7]. The malfunction of Wnt signaling pathway is related to heart diseases including myocardial infarction, cardiac hypertrophy and heart failure[8]. Interestingly, the role of Wnt signaling in cardiovascular disease is still controversial. Some studies report that activation of Wnt pathway can protect against the damage of heart tissue[9], while others demonstrate inhibition of Wnt pathway can improve myocardial hypertrophy, myocardial fibrosis and heart failure[10,11].

Lysine-specific demethylase 4A (KDM4A), also known as JMJD2A, is a member of H3K9me3/me2 and H3K36me3/me2 specific histone lysine demethylase family. As a modulator of gene transcription, KDM4A can promote either transcriptional repression or activation of the genes by its demethylase activity[12]. KDM4A participates in regulation of cell proliferation, differentiation, development, metabolism and other important biological processes[13]. Moreover, KDM4A is involved in the development of cancers. Thus, KDM4A might be a potential target for cancer treatment[14]. Meanwhile, some studies indicate that KDM4A inhibition can block nuclear factor kappa B (NF-κB) activation and functionally recover ischemic stroke[15]. Besides, KDM4A also serves as a prerequisite for modulating NF-κB activity in chromatin remodeling protein BRG1-mediated lipopolysaccharide-induced transcription of pro-inflammatory cytokines in vascular endothelial cells[16]. Reciprocally, high expression of KDM4A causes myocardial hypertrophy in mice underwent a transverse aortic constriction surgery[17].

By completing a network pharmacological analysis, we found that CDDP had complementary mechanisms for statin actions in CHD treatment. Therefore, we hypothesized that CDDP or CDDP combined simvastatin can reduce heart failure. In this study, we constructed mice with dual deficiency of ApoE and low-density lipoprotein receptor (ApoE$^{-/-}$LDLR$^{-/-}$), and fed the mice a high-fat diet (HFD) to induce heart failure while determined the effect of CDDP or CDDP combined simvastatin on hypercholesterolemia/atherosclerosis-induced heart failure. We also attempted to unveil the involved anti-heart injury mechanisms of CDDP and if CDDP can block simvastatin-induced rhabdomyolysis.

2. Materials and methods

2.1. Reagents

2,4-Pyridine dicarboxylicacid (PDCA) was purchased from Selleck Chemicals (Shanghai, China). The antibody information was listed in Supporting Information Table S1. High-fat diet (HFD, 21% fat plus 0.5% cholesterol) was purchased from Medicine Ltd. (Yangzhou, China). Dihydroethidium (DHE) was purchased from Beyotime Biotechnology (Shanghai, China). CDDP, DanShenDuoFenSuan

(DSDF, one main ingredient of CDDP extracted from Danshen) and Xuesaitong (XST, another main ingredient of CDDP extracted from *Panax notoginseng*) were provided by Tasly (Tianjin, China). Brain natriuretic peptide (BNP) and N-terminal pro-BNP ELISA (NT-proBNP) kits were purchased from Elabscience Biotechnology Co., Ltd. (Wuhan, China). Malondialdehyde activity assay kit was purchased from Jiancheng Bioengineering Institute (Nanjing, China). Free fatty acid assay kit was purchased from Beijing Solarbio Science & Technology Co., Ltd. (Beijing, China). Tumor necrosis factor alpha (TNF-α) and interleukin 1 beta (IL-1β) ELISA kits were purchased from Quanzhou Runxin Biotechnology Co., Ltd. (Fujian, China).

2.2. *In vivo studies*

All project procedures for animal studies were approved by the Ethics Committee of Nankai University and strictly performed in compliance with the Guide for the Care and Use of Laboratory Animals (8th edition, The National Academies Press, revised 2011).

Wild type (WT, C57BL/6J), LDL receptor deficient ($LDLR^{-/-}$) and ApoE deficient ($ApoE^{-/-}$) mice with C57BL/6J background were purchased from Vital River Laboratory Animal Technology Co., Ltd. (Beijing, China). $ApoE^{-/-}LDLR^{-/-}$ mice were obtained by crossing $ApoE^{-/-}$ and $LDLR^{-/-}$ mice with gene identification at DNA, mRNA and protein levels. $ApoE^{-/-}LDLR^{-/-}$ mice (~8-week-old) were randomly divided into 5 groups and received the oral treatment: Group 1 (Ctrl group), HFD containing vehicle; Group 2 (LST group) and 3 (HST group), HFD containing simvastatin (ST) at a low (10 mg/kg bodyweight/day, which matches the recommended dose in clinic) and high dose (25 mg/kg bodyweight/day), respectively; Group 4 (CDDP group), HFD containing CDDP (660 mg/kg bodyweight/day); Group 5 (CDDP + ST or CST group), HFD containing CDDP (660 mg/kg bodyweight/day) and the low dose of simvastatin (10 mg/kg bodyweight/day). Wild type mice were fed a normal chow as the normal control. After 16-week treatment, all mice were conducted electrocardiograms (ECG) and echocardiographic test. The left ventricular internal diameter at end-diastole and left ventricular internal diameter at end-systole were calculated based on the echocardiographic results as described[18]. Mice were then euthanized by a lethal dosage of sodium pentobarbital, followed by collection of blood and tissue samples. A piece of fresh heart was used for RNA sequencing (RNA-Seq). Differential expression analysis was assessed using the Bioconductor package edgeR and the genes with $P < 0.05$ and fold change > 2 were identified as significantly differential expression. Gene ontology enrichment analysis was conducted using DAVID (https://david.ncifcrf.gov/)[19]. To validate the role of Wnt signaling pathway in CHD, the gene set enrichment analysis (GSEA) (Version 4.1.0) was used to analyze the data (GSE120774) collected from GEO (https://www.ncbi.nlm.nih.gov/geo/). In addition, a piece of heart from Ctrl (Group 1) or CDDP-treated (Group 4) group was used to determine DNA methylation using the reduced representation bisulphite sequencing methodology as described in the previous study[20].

2.3. *Cell culture*

H9c2 cells, a rat cardiomyocyte cell line, were purchased from ATCC (Rockville, MD, USA) and cultured in DMEM containing 2 mmol/L glutamine, 10% fetal bovine serum, and 50 mg/mL penicillin/streptomycin in an incubator with humidified atmosphere of 95% air plus 5% CO_2 at 37 °C. H9c2 cells at ~90% confluence received the indicated treatment in serum-free medium. NovoCell-Cardiomyocytes (iPSC-CM) cells, differentiated from the induced pluripotent stem cells, were purchased from Help Stem Cell Innovations Co., Ltd. (Nanjing, China), and cultured in the specific cardiomyocyte culture medium (Code# Help4001-2, Help Stem Cell Innovations Co., Ltd.). RAW 264.7 cells, a murine macrophage cell line, were purchased from ATCC (Rockville, MD, USA) and cultured in RPMI 1640 medium containing 1% penicillin/streptomycin, 1% glutamine and 10% fetal bovine serum in an incubator with humidified atmosphere of 95% air plus 5% CO_2 at 37 °C.

2.4. *Network pharmacology analysis*

The chemical structure similarity was estimated as follows. The Simplified Molecular Input Line Entry System (a chemical notation that allows a user to represent a chemical structure in a way that can be used by computer) of FDA-approved drugs and CDDP components were collected from PubChem (https://pubchem.ncbi.nlm.nih.gov/) and converted to Morgan fingerprints. The structure-based similarity was calculated by Tanimoto coefficient among those fingerprints of molecules using RDKit modules (v2020.09.01). The hierarchical clustering of molecules was performed by R package hClust based on the similarity matrix of chemical structure. The iTOL (https://itol.embl.de/) was used to visualize the clustering tree.

The correlation between drug targets and disease genes was completed by the following method. Totally, 1974 genes associated with CHD were obtained from DisGeNET with the keywords of "coronary artery disease" and "coronary heart disease"[21]. 140 CDDP-targeted genes were obtained from publications, and 44 genes targeted by FDA-approved drugs were collected from DrugBank, PubChem and STITCH (http://stitch.embl.de/)[22,23]. To evaluate the correlation between CDDP combined simvastatin and CHD, we merged the two sets of targets into a non-redundant target set for subsequent analysis. From perspective of the network propagation, the correlation between drug's target and genes associated with disease was evaluated. First, the drug targets and disease genes were taken as the seed genes respectively to run Random Walk with Restart algorithm using STRING as background network, which was performed in R package *dnet* (version 1.1.7) with 0.75 of the restart probability, to obtain the corresponding influence score vector. Pearson correlation coefficient of the two score vectors (Cor) was then calculated according to Eq. (1), and the Z-score was used to evaluate the significance of the correlation by conducting a permutation test.

$$\text{Z-score} = \frac{\text{Cor} - E(\text{Cor})}{\delta(\text{Cor})} \quad (1)$$

E(Cor) and δ(Cor) are the mean and standard deviation of the Pearson correlation coefficients between influence score vector of drug targets and those of 1000 groups of random contrast disease genes, each of which contained the same number of randomly selected proteins as the disease seed nodes.

2.5. *Determination of protein and mRNA expression*

After treatment, total protein was extracted from mouse tissues, H9c2, iPSC-CM cells or RAW 264.7 macrophages and used to determine protein expression by Western blot as described[24]. All the Western blot images were scanned and the density of bands was

semi-quantitatively analyzed. The statistical results of band density analysis were presented in Supporting Information Tables S2 and S3.

Total RNA was extracted from mouse heart or H9c2 cells using Trizol Reagent (Zomanbio, Beijing, China). mRNA expression was determined by quantitative real-time PCR (qRT-PCR) with AceQ qPCR SYBR Green Master Mix (Vazyme, Nanjing, China) and the primers with sequences listed in Supporting Information Table S4. The mRNA levels were normalized with *Gapdh* mRNA levels in the corresponding samples.

2.6. Oxygen and glucose deprivation (OGD)

Cells were cultured in OGD condition (in a tank filled with a gas mixture of 95% N_2 plus 5% CO_2 at 37 °C and in serum-free medium lacking glucose) or in OGD condition plus treatment of CDDP, CDDP components (DSDF or XST), or the combination of CDDP/CDDP component and PDCA for 12 h. Cells cultured in normal condition (95% air plus 5% CO_2 at 37 °C and medium containing glucose) were used as control. After treatment, the cell viability was determined by the Cell Counting Kit-8 Assay Kit (Yeasen, Shanghai, China). Cellular protein and RNA were extracted to detect expression of the indicated molecules by Western blot and qRT-PCR, respectively. To determine the role of KDM4A in CDDP-protected OGD-induced cell toxicity, cells were transfected with si*KDM4A* or si*Ctrl* (100 nmol/L, purchased from Tsingke Biotechnology Co., Ltd., Beijing, China) using Lipofectamine 3000 Transfection Reagent (Invitrogen), and then continued the indicated treatment for 12 h.

2.7. Histopathologic assay

All tissues collected were soaked in 10% formalin for 48 h, dehydrated, embedded in paraffin, and then cut into 5 μm sections for hematoxylin−eosin (HE) staining. Meanwhile, Masson trichrome and picrosirius red staining were performed on heart sections to assess collagen content and fibrosis. After drying, all the slides were photographed.

2.8. Determination of hepatic lipid content

Liver samples were fixed, dehydrated, embedded in OCT and cut into 5 μm frozen sections. The sections were incubated in phosphate-buffered saline (PBS) for 1 h followed by staining with oil red O solution (3 mg/mL in 60% isopropanol) for 60 min. After washed with distilled water, the sections were stained with alum hematoxylin solution for 50 s for nuclei, followed by washing with PBS and photograph.

To quantify hepatic triglyceride (TG) content, a piece of liver (∼30 mg) was homogenized in 1 mL PBS, then 900 μL homogenate was used to extract total lipids for TG quantitative analysis, and the rest of homogenate was used to determine protein content for TG normalization.

2.9. Determination of ROS levels

Fresh mouse heart samples were washed with PBS and then quickly frozen in liquid nitrogen. The frozen heart tissues were embedded into OCT, and then cut into 5 μm frozen sections. After soaked in PBS for 1 h at room temperature, the sections were incubated with 5 μmol/L DHE for 30 min at 37 °C in dark, followed by washing with PBS and photographed by Leica DM5000B microscope (Leica Microsystems, Wetzlar, Germany) or used for ROS detection by the Reactive Oxygen Species Fluorometric Assay Kit (Elabscience, Wuhan, China). The fluorescence intensity was quantified using the Image J software.

2.10. Meta-analysis

Three mainstream medical databases, PubMed, CNKI and WANFANG, were searched. The timeframe used for database queries was from the earliest indexed studies to July, 2021. The search words included are "Compound Danshen Dripping Pills combined with statins". The volunteers were divided into control group and experimental group. The control group was treated with statins, and the experimental group was treated with CDDP combined statins. The main outcomes included: lipid profiles (TG, total cholesterol, low-density lipoprotein cholesterol, high-density lipoprotein cholesterol), left ventricular ejection fraction and left ventricular end diastolic diameter. The following studies were excluded from the meta-study: (1) duplicate studies; (2) non-randomized trials; (3) case reports, reviews, systematic reviews and abstracts; (4) the basic treatment of the control group and the experimental group are inconsistent. Two researchers selected the papers independently. The included literature research data were statistically analyzed by Revman 5.4 software. Q test and I^2 value were used to analyze the heterogeneity among the included studies. Mean difference, odds ratio and 95% CI were used as the analysis statistics, and $P \leq 0.05$ is considered of statistically significant.

2.11. Analysis of KDM4 kinase activity

The inhibitory effect of CDDP on KDM4 activity was performed with an *in vitro* kinase assay system. The detailed information for the assay, such as the procedure, data analysis, and calculation of IC_{50}, is described in the Supporting Information.

2.12. Molecular modeling

Molecular docking was used to display the non-covalent bond and the binding posture between KDM4A and CDDP components. The analytical protein structure of KDM4A was extracted from the RCSB protein database[25] using the protein prepared wizard module of the Schrödinger Suite (v2017, Schrödinger Inc., NY, USA) to remove all the water of crystal molecules, rectify side chains lacking atoms, add hydrogen atoms and specify protonation state and partial charge using OPLS_2005 force field. Finally, the minimization of crystal structure was terminated when the root mean square deviation of non-hydrogen atom reached a maximum cutoff of 0.30 Å. CDDP components were prepared using Ligprep module of the Schrödinger Suit, adding hydrogen atoms, converting structures from 2D to 3D, generating stereoisomers, and determining the ionization state at pH = 7.0 ± 2.0 with Epik module. Receptor grid files were generated by the original ligand of the protein with the prepared receptor structure, and the docking between CDDP component and receptor was carried out using Glide XP score.

2.13. Statistical analysis

All data are presented as mean ± standard error of mean (SEM) with indicated "*n*" value. Multi-group data followed normal distribution were analyzed by ANOVA with Tukey post-test using GraphPad Prism (Version 7.0). Differences were considered statistically significant if $P < 0.05$.

3. Results

3.1. Identification of the pharmacological mechanisms of CDDP on CHD

CDDP contains many components with different kinds of bioactivities[26]. To identify the pharmacological mechanisms for the therapeutic actions of CDDP/CDDP components on CHD, we collected 67 molecules of the simplified molecular input line entry system strings. These molecules consist of 45 drugs approved by FDA of USA representing different mechanisms of actions (MoAs) for CHD treatment and 22 CDDP components which include the main components found in the blood after CDDP administration and the bioactive equivalent components (Supporting Information Tables S5 and S6)[26,27]. We analyzed the chemical structure similarity among CDDP components and the FDA-approved drugs. The hierarchical clustering of chemical compounds based on the structural similarity shows that CDDP components with similar chemical structures largely clustered together, while FDA-approved drugs within the same MoA almost clustered together also. However, CDDP components did not cluster with any of FDA-approved drug (Supporting Information Fig. S1A), indicating no shared structural similarity between the two groups.

The MoAs of a drug can be predicted by its gene expression signatures in Genetic Profileactivity Relationship (GPAR) platform (an online collaborative tool to model and predict MoAs of drugs *via* deep learning)[28]. The gene expression signatures of CDDP were obtained from CDDP-treated human cardiomyocytes and used to predict the MoAs of CDDP in GPAR platform. The results show that the MoAs of CDDP are quite different from that of 3-hydroxy-3-methylglutaryl-coenzyme A reductase inhibitors, statins including simvastatin. The GPAR score of simvastatin is 0.0138, ranked 55th out of 83, in terms of MoA similarity (Fig. S1B). Moreover, the combination of CDDP and simvastatin is more significantly correlated with CHD than CDDP or simvastatin alone (Fig. S1C), that might be attributed to the complementarity between CDDP and simvastatin. It also suggests that combined CDDP and simvastatin may provide better protection than CDDP or simvastatin alone against CHD.

3.2. CDDP protects ApoE$^{-/-}$LDLR$^{-/-}$ mice against hypercholesterolemia/atherosclerosis-induced myocardial injury

Coronary atherosclerosis is the most important primary etiologic factor for heart failure[29]. Lack of ApoE or LDLR expression in mice can accelerate the development of HFD-induced hypercholesterolemia and atherosclerosis. However, it is hardly to observe coronary artery plaques or heart injury in ApoE$^{-/-}$ or LDLR$^{-/-}$ mice, which may be attributed to lack of chronic myocardial ischemia[30,31]. We speculated that combined ApoE and LDLR deficiency may cause additional cholesterol metabolic disorders, therefore, under HFD feeding, ApoE and LDLR dual deficient (ApoE$^{-/-}$LDLR$^{-/-}$) mice can develop not only hypercholesterolemia and atherosclerosis in aortal artery, but also coronary arterial lesions and heart failure. By crossing ApoE$^{-/-}$ and LDLR$^{-/-}$ mice, we obtained ApoE$^{-/-}$LDLR$^{-/-}$ mice and confirmed no ApoE and LDLR expression by genotyping, RNA-Seq, Western blot and qRT-PCR (Supporting Information Fig. S2A–S2D).

ApoE$^{-/-}$LDLR$^{-/-}$ mice were scheduled the treatment as indicated in Fig. 1A. After 16-week treatment, aortic lesions were determined by oil red O staining. Fig. 1B and C show HFD induced severe *en face* aortic lesions in ApoE$^{-/-}$LDLR$^{-/-}$ mice. Treatment of ApoE$^{-/-}$LDLR$^{-/-}$ mice with simvastatin reduced lesions in a dose-dependent manner. Interestingly, CDDP or plus the low dose of simvastatin reduced lesions at a comparable level to that by the high dose of simvastatin. The effect of simvastatin, CDDP or CDDP plus the low dose of simvastatin on aortic root lesions was similar to that on *en face* lesions (Fig. S2E). These results demonstrate that CDDP has the potent anti-atherogenic properties.

All mice were conducted ECG and echocardiogram tests before sacrifice and tissue collection. Compared with WT mice, ECG shows the depression of ST-segment in HFD-fed ApoE$^{-/-}$LDLR$^{-/-}$ mice, which should be contributed by decreased ejection fraction and fractional shortening (Fig. 1D–F). It also indicates that heart dysfunctions occurred to HFD-fed ApoE$^{-/-}$LDLR$^{-/-}$ mice. In contrast, high dose of simvastatin (HST), CDDP alone or CDDP plus the low dose of simvastatin significantly ameliorated these dysfunctions since both ST-segment depression and decreased ejection fraction/fractional shortening were restored to normal (Fig. 1E and F). However, the low dose of simvastatin alone had little protective effect. Thus, the data above demonstrate that CDDP or CDDP plus the low dose of simvastatin substantially protects ApoE$^{-/-}$LDLR$^{-/-}$ mice against HFD-induced atherosclerosis and heart injury.

3.3. CDDP reduces HFD-induced cardiac dysfunction in ApoE$^{-/-}$LDLR$^{-/-}$ mouse heart

Normally, the cardiac dysfunction is associated with cardiac hypertrophy. Compared with WT mice, HFD-fed ApoE$^{-/-}$LDLR$^{-/-}$ mice had increased ratio of heart weight to body weight, which was substantially attenuated by simvastatin, CDDP or their combination (Fig. 2A), indicating the treatment reduced cardiac hypertrophy in HFD-fed ApoE$^{-/-}$LDLR$^{-/-}$ mice. Indeed, the protection against cardiac hypertrophy by the treatment, particularly by CDDP plus the low dose of simvastatin, was further confirmed by HE staining of heart sections (Fig. 2B and C).

The levels of serum creatine kinase, lactate dehydrogenase, α-hydroxybutyrate dehydrogenase, BNP and NT-proBNP reflect the severity of myocardial injury. Compared with WT mice, all of these parameters were potently increased in HFD-fed ApoE$^{-/-}$LDLR$^{-/-}$ mice, but they were substantially reduced by the treatment, particularly by CDDP or CDDP plus the low dose of simvastatin (Fig. 2D–H).

In addition to BNP, atrial natriuretic factor (ANF) is another member of the polypeptide family produced and secreted by heart atria and demonstrates diuretic and natriuretic activity. BNP and ANF expression are activated associated with heart failure. Beta myosin heavy chain (β-MHC) is an MHC isoform and expresses at a low level in adult heart physiologically. Increased β-MHC in the heart results in decreased myofibrillar Ca^{2+}-activated ATPase activity and systolic function. Consistently, increased *Anf*, *Bnp* and *β-Mhc* mRNA expression confirmed the cardiac injury in HFD-fed ApoE$^{-/-}$LDLR$^{-/-}$ mouse heart. However, simvastatin reduced activation of these molecules in a dose-dependent manner, while CDDP or CDDP plus the low dose of simvastatin fully normalized their expression (Fig. 2I).

The prolonged heart inflammation can lead to myocardial remodeling and cardiac myocyte apoptosis. The results of HE staining indicate severe inflammatory cell infiltration and myocardial structural disorder in HFD-fed ApoE$^{-/-}$LDLR$^{-/-}$ mouse heart. The low dose of simvastatin moderately while the high dose of simvastatin, CDDP or CDDP plus the low dose of simvastatin, potently

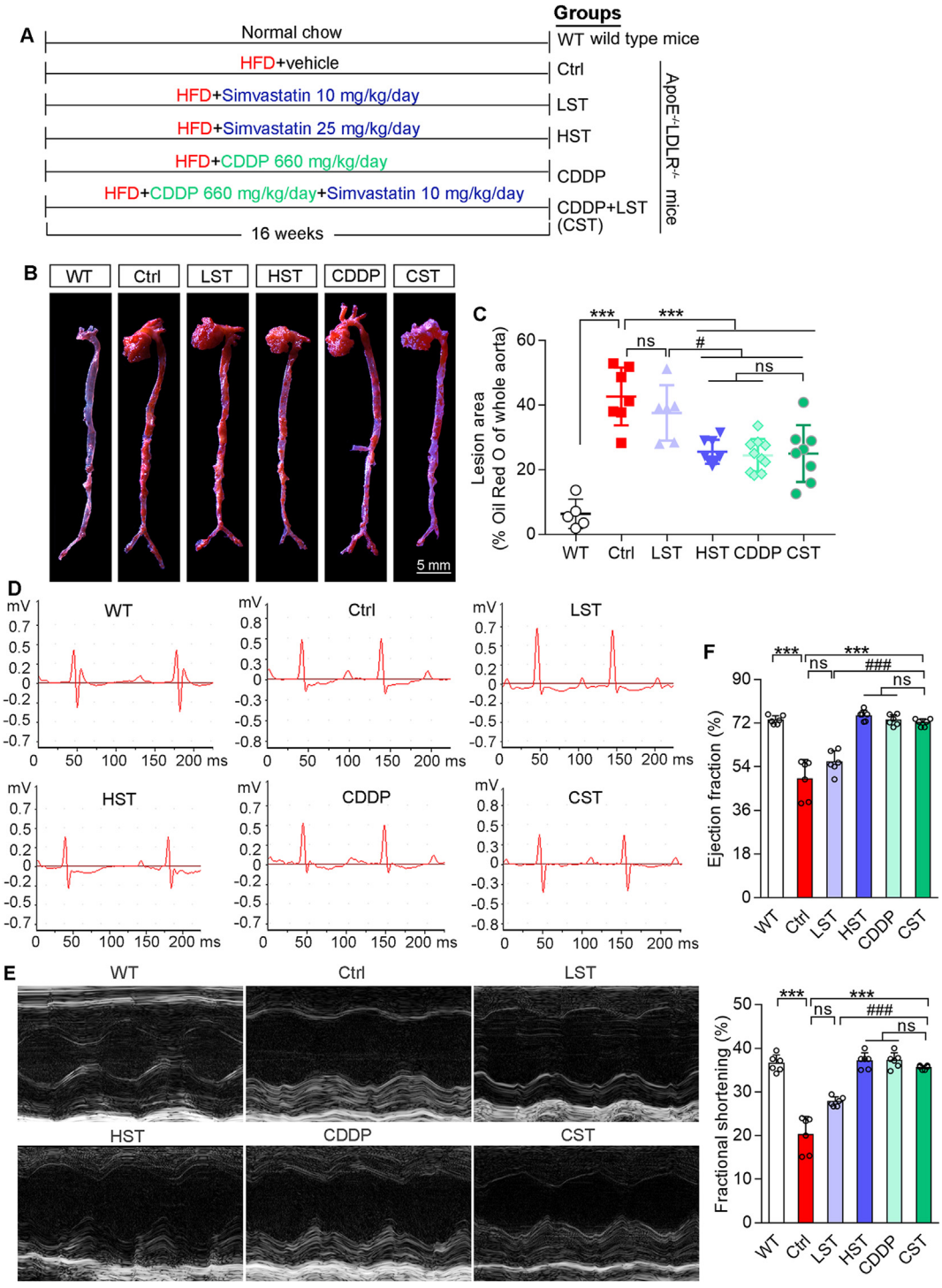

Figure 1 CDDP protects ApoE$^{-/-}$LDLR$^{-/-}$ mice against HFD-induced myocardial injury. (A) Mice were assigned to the groups and received the indicated treatment. After 16-week treatment, mice were conducted the following assays. (B, C) Aortic *en face* lesions were determined by oil red O staining with quantitative analysis of lesion areas. (D, E) The representative pictures of mouse ECG and echocardiographic test. (F) Ejection fraction and fractional shortening were calculated based on echocardiographic test. The data are shown as mean ± SEM. $^{***}P < 0.001$ *vs*. Ctrl; $^{\#}P < 0.05$, $^{\#\#\#}P < 0.001$ *vs*. LST; ns: not significantly different between indicated groups. $n = 5$–9 mice/group. ECG: electrocardiograms.

reduced infiltration of inflammatory cells (Fig. 2J), indicating the anti-heart inflammation is another cardiac protective property of CDDP. Both picrosirius red and Masson trichrome staining display significant collagen deposition in HFD-fed ApoE$^{-/-}$LDLR$^{-/-}$ mouse heart. While the high dose of simvastatin, CDDP or CDDP plus the low dose of simvastatin markedly reduced myocardial fibrosis (Fig. 2K and L). Correspondingly, increased mRNA expression of the fibrosis-related genes, such as transforming growth factor beta (*Tgf-β*), alpha smooth muscle actin and collagen I alpha 1 in HFD-fed ApoE$^{-/-}$LDLR$^{-/-}$ mouse heart was significantly abrogated by the high dose of simvastatin, CDDP or CDDP plus the low dose of simvastatin (Fig. 2M). Thus, the data above demonstrate that

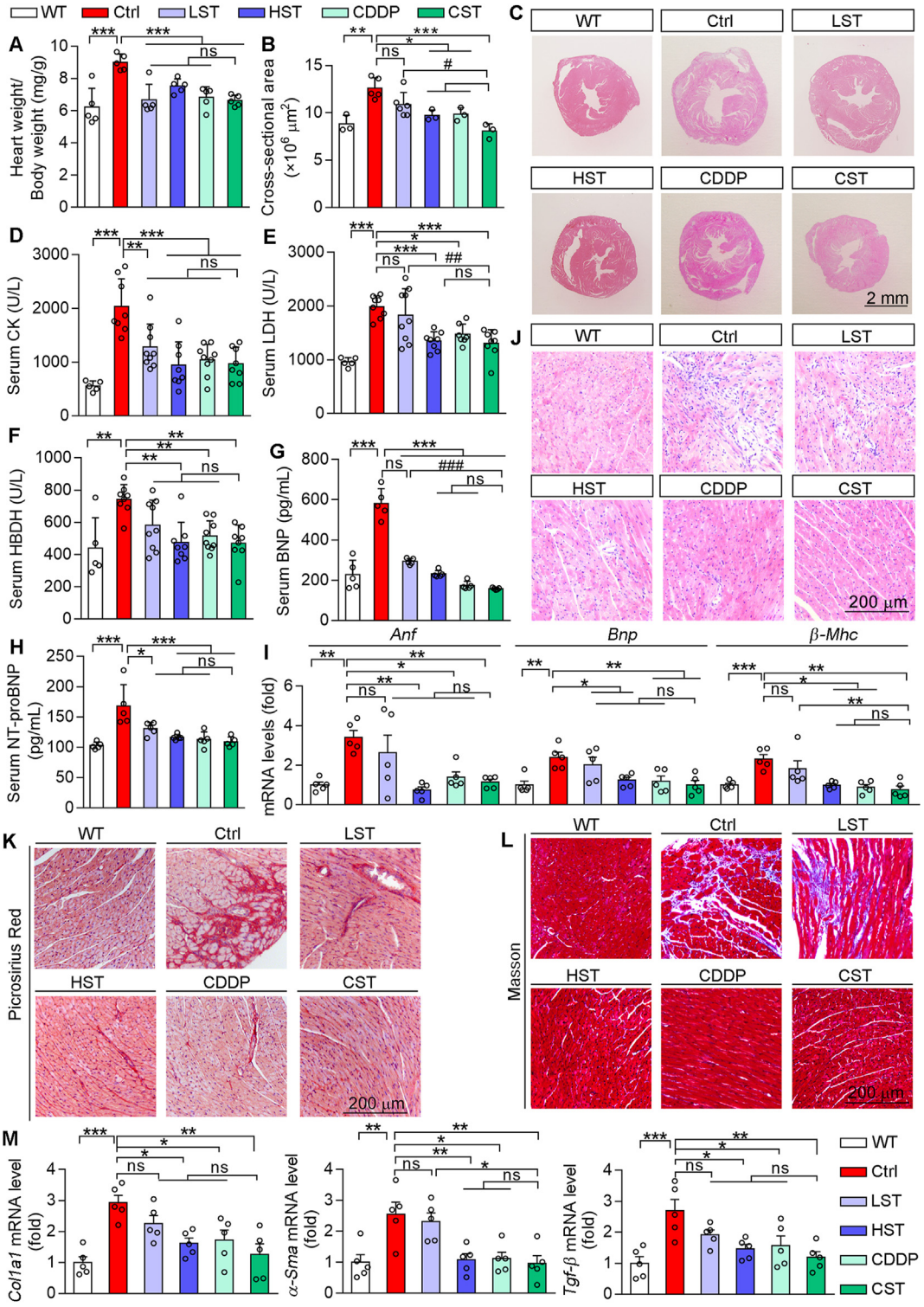

Figure 2 CDDP treatment improves HFD-induced cardiac dysfunctions in ApoE$^{-/-}$LDLR$^{-/-}$ mice. (A) The ratio of heart weight to body-weight ($n = 5$). (B, C) HE staining of mouse heart cross sections with quantitation of the cross-sectional area. (D−H) Levels of serum CK, LDH, BNP, HBDH and NT-proBNP were determined by assay kits ($n = 5$−8). (I) Expression of *Anf*, *Bnp* and *β-Mhc* mRNA was determined by qRT-PCR ($n = 5$). (J) HE staining of mouse heart section to determine infiltration of inflammatory cells. (K, L) Picrosirius red staining and Masson trichrome staining of heart sections. (M) mRNA levels of *Col1a1*, *α-Sma* and *Tgf-β* were determined by qRT-PCR ($n = 5$). The data are shown as mean ± SEM. $^{*}P < 0.05$, $^{**}P < 0.01$, $^{***}P < 0.001$; $^{\#}P < 0.05$, $^{\#\#\#}P < 0.001$; ns: not significantly different between indicated groups. ANF, atrial natriuretic factor; CK, creatine kinase; *α-Sma*, alpha smooth muscle actin; *Col1a1*, collagen type I alpha 1 chain; HDBH, α-hydroxybutyrate dehydrogenase; LDH, lactate dehydrogenase; NT-proBNP, N-terminal pro-brain natriuretic peptide.

CDDP or CDDP plus the low dose of simvastatin substantially protects ApoE$^{-/-}$LDLR$^{-/-}$ mice against HFD-induced heart injury.

3.4. *CDDP inactivates Wnt pathway to reduce heart injury in HFD-fed ApoE$^{-/-}$LDLR$^{-/-}$ mice*

To determine the mechanisms of CDDP reducing myocardial injury, we conducted RNA-Seq analysis with mouse heart RNA, and compared the expression patterns between HFD-fed ApoE$^{-/-}$LDLR$^{-/-}$ (Ctrl) and wild type (WT) or CDDP-treated HFD-fed ApoE$^{-/-}$LDLR$^{-/-}$ (CDDP) mice (Fig. 3A). The results show that expression of 481 genes was significantly changed between HFD-fed ApoE$^{-/-}$LDLR$^{-/-}$ and WT mice with 356 genes up-regulated and 125 down-regulated. Meanwhile, expression of 237 genes was significantly changed between CDDP-treated HFD-fed ApoE$^{-/-}$LDLR$^{-/-}$ and HFD-fed ApoE$^{-/-}$LDLR$^{-/-}$ mice with 197 genes up-regulated and 40 genes down-regulated. Interestingly, 87 genes were commonly changed in both comparison groups (Fig. 3B), furthermore, 70 of them changed in Ctrl group were reversed by CDDP treatment (Fig. 3C).

The results of a gene ontology analysis on those 70 genes show that they are mainly enriched in Wnt pathway (Fig. 3D and Supporting Information Fig. S3A). Many studies have demonstrated that Wnt pathway is drastically activated during cardiac remodeling and heart failure[32,33]. Consistently, we observed that Wnt pathway was activated in HFD-fed ApoE$^{-/-}$LDLR$^{-/-}$ mouse heart since several anti-Wnt pathway molecules[7], such as Wnt inhibitory factor 1 (*Wif1*), secreted frizzled related protein 4 or 5 (*Sfrp4/5*), NKD inhibitor of Wnt signaling pathway 1 (*Nkd1*) and Dickkopf Wnt signaling pathway inhibitor 2 (*Dkk2*), were inhibited. However, the inhibition of these anti-Wnt pathway molecules was re-activated by simvastatin, CDDP or CDDP plus the low dose of simvastatin with most potent effect by CDDP alone (Fig. 3E).

Consistently, compared with WT mice, expression of SFRP4/5, WIF1, NKD1 and DKK2 protein and mRNA in HFD-fed ApoE$^{-/-}$LDLR$^{-/-}$ mouse heart was reduced, accompanied by increased β-catenin expression, a molecule with an independent role in activation of Wnt target gene transcription (Fig. 3F and G). However, changes in these molecules in HFD-fed ApoE$^{-/-}$LDLR$^{-/-}$ mouse heart were fully restored by CDDP or CDDP plus the low dose of simvastatin (Fig. 3F and G).

The relationship between Wnt pathway and CHD was further assessed by the GSEA on the array data obtained with epicardial and subcutaneous adipose tissue in CHD patients (GSE120774 in GEO)[34]. Similar to our mouse model, the GSEA results show Wnt pathway is also significantly activated in CHD patients (Fig. S3B and S3C).

Bone morphogenetic protein 3 (BMP3), a member of TGF-β family, can reduce cardiovascular risk and pathological heart remodeling[35]. Interestingly, Wnt can activate TGF-β expression, which negatively regulates BMP3 expression[36]. In addition to *Tgf-β* activation (Fig. 2M), inhibition of BMP3 was observed in HFD-fed ApoE$^{-/-}$LDLR$^{-/-}$ mouse heart, and either activated *Tgf-β* or inhibited BMP3 was restored by CDDP or CDDP plus the low dose of simvastatin (Figs. 2M and 3F), further suggesting the importance of inactivated Wnt pathway in protection against heart failure by CDDP.

Heart injury is closely related to myocardial ischemia, which is mainly caused by lack of oxygen and energy supplementation[37]. We applied an OGD model to H9c2 and iPSC-CM cells to determine the effect of CDDP on OGD-induced injury to cardiomyocytes. OGD condition reduced cell viability obviously while CDDP blocked the reduction in a concentration-dependent manner (Supporting Information Fig. S4A and S4B). In H9c2 cells, OGD inhibited expression of SFRP4/5, NKD1, BMP3, WIF1, DKK2 protein while activated β-catenin protein expression, and these changes were reversed by CDDP (Fig. S4C). The similar changes were observed in iPSC-CM cells except the opposite changes of β-catenin happened (Fig. S4D). Correspondingly, OGD-inhibited *Sfrp4/5*, *Nkd1*, *Wif1* and *Dkk2* mRNA expression in H9c2 cells was blocked by CDDP (Fig. S4E). Thus, the protection of cardiomyocytes against OGD-induced injury *in vitro* by CDDP is also related to inhibition of Wnt pathway.

Taken together, the data above demonstrate that CDDP or CDDP plus the low dose of simvastatin substantially protects ApoE$^{-/-}$LDLR$^{-/-}$ mice against HFD-induced heart injury by regulating Wnt pathway.

3.5. *CDDP inactivates KDM4 pathway to attenuate inflammation and oxidative stress in HFD-fed ApoE$^{-/-}$LDLR$^{-/-}$ mice*

Inflammation plays a key role in the progression of heart failure[38]. Initially, we determined that the high dose of simvastatin, CDDP or CDDP plus the low dose of simvastatin reduced the levels of TNF-α and IL-1β in serum (Fig. 4A), which indicate that the anti-inflammation can be another important mechanism for CDDP or CDDP plus the low dose of simvastatin in anti-heart injury. The KDM4 family is a subfamily of histone lysine demethylases including several members, such as KDM4A and KDM4E. In addition to cancers[39], inhibition of KDM4A also reduces ischemic stroke by inhibiting inflammatory factors including TNF-α and IL-1β by regulating phosphorylation of NF-κB p65 (p-P65)[15]. Consistently, we determined that the high dose of simvastatin, CDDP or CDDP plus the low dose of simvastatin reduced expression of P65, p-P65, TNF-α and IL-1β at protein or mRNA levels (Fig. 4B and Supporting Information Fig. S5A). Interestingly, CDDP or CDDP plus the low dose of simvastatin but not simvastatin alone reduced KDM4 expression (Fig. 4B), indicating that the anti-inflammation by CDDP, not simvastatin, might be completed through inactivation of KDM4A.

In addition to expression, the effect of CDDP on KDM4 activity was also determined. Similar to expression, the results of *in vitro* kinase assay demonstrate that CDDP reduced KDM4A (IC_{50} = 0.0065 mg/mL, Fig. 4C) and KDM4E (IC_{50} = 0.0074 mg/mL, Fig. S5D) activity. Furthermore, the inhibitory effect of CDDP on KDM4 activity was confirmed mainly accomplished by its main components extracted from Radix Salviae (Danshen), not from *Panax notoginseng* (Fig. S5B, S5C, S5F and S5G).

The molecular docking demonstrates the interaction between CDDP components and KDM4A. Compared with 3-[(4-fluorobenzyl) amino] pyridine-4-carboxylic acid (the KDM4A co-crystal ligand), the results of 2D structure display that several CDDP main components can well occupy the binding site in KDM4A with a comparable or even a better docking score than this ligand (Fig. 4D−F), further confirming the inhibitory effect of CDDP on KDM4A activity.

Consistent with the results in mice, OGD also activated expression of KDM4A, p-P65, TNF-α and IL-1β protein in H9c2 and iPSC-CM cells. However, CDDP effectively reversed these changes (Fig. 4G). OGD-activated *Tnf-α* and *Il-1β* mRNA expression was potently inhibited by CDDP in H9c2 cells (Fig. S5H). To further verify that inhibition of inflammation by

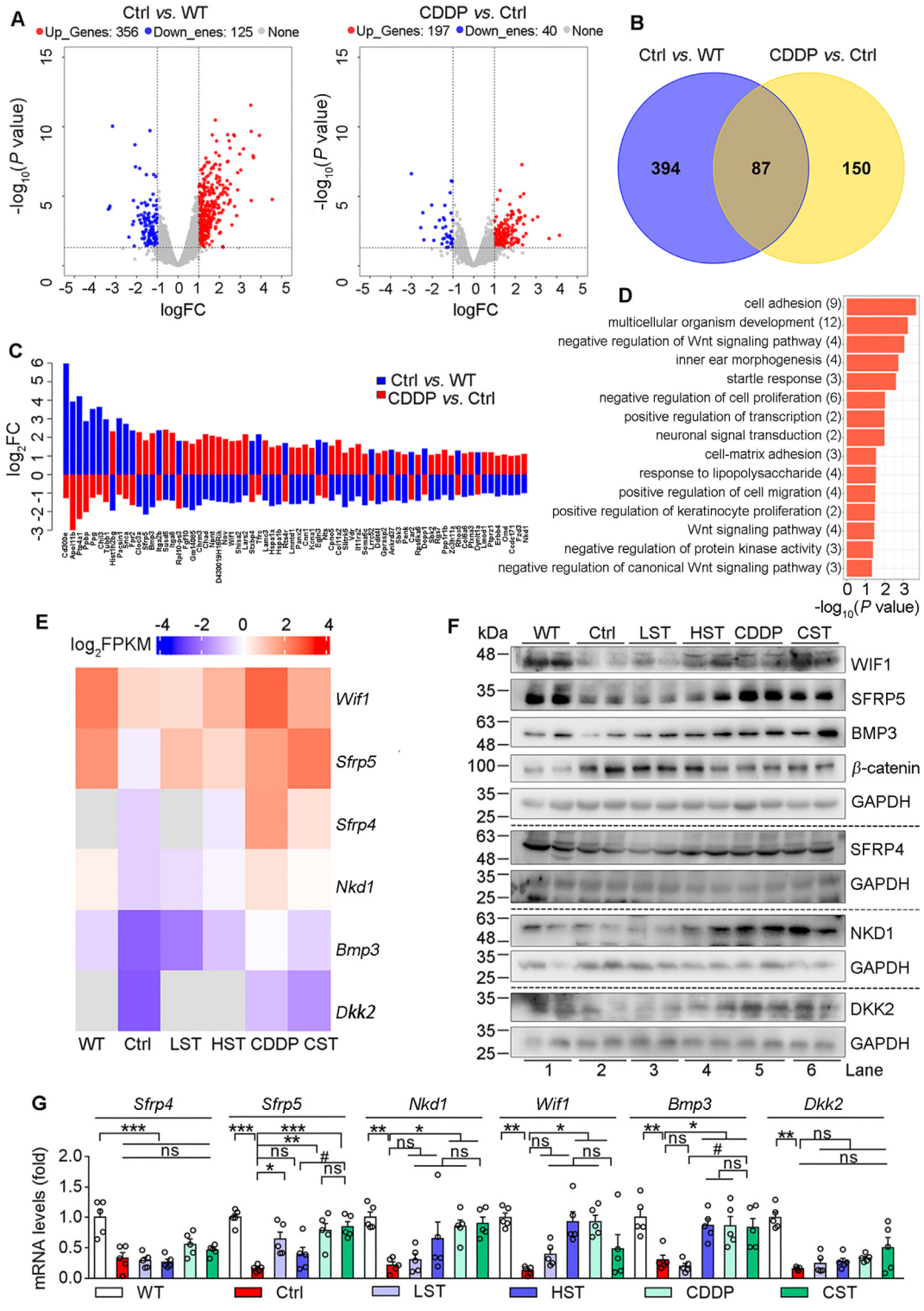

Figure 3 CDDP protects ApoE$^{-/-}$LDLR$^{-/-}$ mice against HFD-induced heart injury by inactivating Wnt pathway. Heart tissues of wild type (WT) mice, HFD-fed (Ctrl) and HFD-fed plus CDDP treated (CDDP) ApoE$^{-/-}$LDLR$^{-/-}$ mice (3 mice/group) in Fig. 1 were conducted RNA-seq analysis. (A) The volcano plot shows the genes expressing differently between Ctrl and WT or CDDP and Ctrl. Significantly different expression genes (DEGs) were defined by threshold ($P < 0.05$) and [$\log_2$ (Fold Change/FC) > 1]. Upregulated genes were marked in red and downregulated genes in blue. (B) Venn diagram shows comparison of DEGs between Ctrl and WT or CDDP and Ctrl group, and 87 DEGs were overlapped. (C) Among the 87 DEGs, 70 of them were reversed by CDDP treatment. (D) The reversible 70 DEGs were classified by GO enrichment analysis. (E) Heatmap shows expression profiles of the reversible DEGs related to Wnt signaling pathway. (F) Protein expression of BMP3, WIF1, SFRP5, SFRP4, NKD1, DKK2, β-catenin was determined by Western blot. (G) mRNA levels of *Bmp3*, *Wif1*, *Sfrp5*, *Sfrp4*, *Nkd1*, *Dkk2* were determined by qRT-PCR ($n = 5$). The data are shown as mean ± SEM. $^{*}P < 0.05$, $^{**}P < 0.01$; $^{***}P < 0.001$; $^{\#}P < 0.05$; ns: not significantly different between indicated groups. GO: gene ontology.

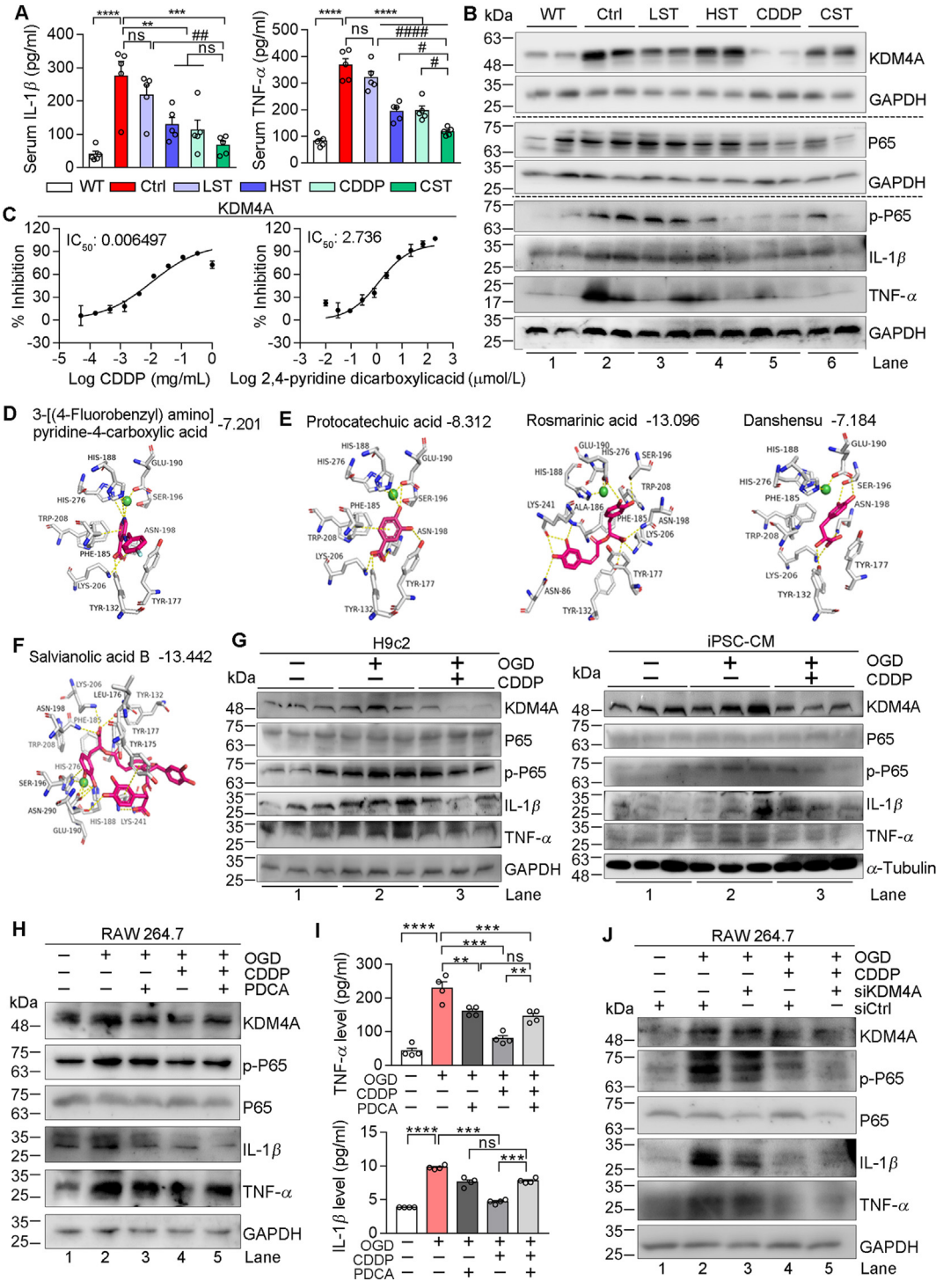

Figure 4 CDDP inhibits KDM4A to decrease inflammation. The levels of serum TNF-α and IL-1β (A) and protein expressions of KDM4A, P65, p-P65, IL-1β and TNF-α in heart samples (B) of mice in Fig. 1 were determined by assay kits ($n = 5$) and Western blot, respectively. (C) Inhibition of KDM4A activity by CDDP was determined by the *in vitro* enzymatic activity assay system. (D−F) Molecular docking of KDM4A with the co-crystal ligand (D) or CDDP components (E, F) with the corresponding docking score shown on the top of each figure. (G−J) H9c2, iPSC-CM or RAW 264.7 cells were cultured in normal culture condition, OGD condition or OGD condition plus treatment of CDDP (G) 500 μg/mL in H9c2, 1000 μg/mL in iPSC-CM), PDCA (1 μmol/L) or CDDP plus PDCA (1 μmol/L) (H, I) for 12 h. RAW 264.7 cells in normal culture condition or OGD condition were transfected with control siRNA (si*Ctrl*) or siRNA against KDM4A (si*KDM4A*), followed by CDDP treatment (J) for 12 h. After treatment, cells (G, H, J) and treatment medium (H) were collected and used to conduct the following assays: expressions of KDM4A, P65, p-P65, IL-1β and TNF-α protein were determined by Western blot, and levels of TNF-α, IL-1β in cell treatment medium were determined by ELISA assay kits. The data are shown as mean ± SEM. $^{*}P < 0.05$, $^{**}P < 0.01$, $^{***}P < 0.001$, $^{****}P < 0.0001$; $^{\#}P < 0.05$, $^{\#\#}P < 0.01$; ns: not significantly different between indicted groups.

CDDP is mainly through inactivation of KDM4A, we treated RAW 264.7 macrophages with PDCA (a KDM4A chemical inhibitor) or CDDP. We found either PDCA or CDDP reversed OGD-induced expression of KDM4A, p-P65, TNF-α and IL-1β protein in cells, and the levels of TNF-α and IL-1β in treatment medium. However, the co-treatment of CDDP and PDCA did not show additive inhibition on expression of these pro-inflammatory factors, indicating they use the same action pathway (Fig. 4H and I). The similar results were obtained when expression of KDM4A in RAW 264.7 macrophages was reduced by KDM4A siRNA (si*KDM4A*) while received CDDP treatment (Fig. 4J). Furthermore, we treated cells with the main components of CDDP (DSDF and XST), and obtained the consistent results with CDDP on expression of KDM4A and pro-inflammatory factors (Fig. S5I–S5N), indicating that the anti-inflammation by CDDP main components is also related to inactivation of KDM4A.

KDM4A is a histone demethylase enzyme, indicating it may influence some signaling pathways by regulating demethylation of the target gene DNA, such as transcription factors. For instance, the methylation of *Rela* (*P65*) can negatively regulate the transcriptional activity of NF-κB to inhibit inflammation. To further unveil if the anti-inflammation CDDP is associated with KDM4A-regulated DNA demethylation, we initially determined the global DNA methylation of the heart samples of HFD-fed ApoE$^{-/-}$LDLR$^{-/-}$ mice (Ctrl group) and the mice received CDDP treatment (CDDP group). Compared with Ctrl group, a slight but not significant increase of global DNA methylation was observed in CDDP-treated mouse heart (Supporting Information Fig. S6A and S6B), which might be attributed to partial inhibition of histone demethylases including KDM4A by CDDP treatment. The further detailed analysis on the results of methylation showed that the CG promoter methylation of *P65* was increased in CDDP group (Fig. S6C), which was associated with decreased *P65* mRNA expression (Fig. S5A). These data indicate that CDDP may inhibit KDM4A to increase CG promoter DNA methylation of *P65*, thereby suppressing P65 expression/phosphorylation and its function on inflammation.

ROS can promote cardiac fibrosis and make substantial contributions to the development of heart failure[40,41]. By DHE staining and malondialdehyde test, we found that high dose of simvastatin, CDDP or CDDP plus the low dose of simvastatin significantly reduced ROS levels in HFD-fed ApoE$^{-/-}$LDLR$^{-/-}$ moue heart (Fig. 5A–C). Meanwhile, accumulated free fatty acid in HFD-fed ApoE$^{-/-}$LDLR$^{-/-}$ mouse heart, which may stimulate ROS production, was also eliminated by the high dose of simvastatin, CDDP or CDDP plus the low dose of simvastatin (Supporting Information Fig. S7A).

Nuclear factor erythroid 2 related factor 2 (NRF2), the key sensor of oxidative stress, activates transcription of antioxidant genes including superoxide dismutase 2 (SOD2), catalase (CAT), and glutamate-cysteine ligase catalytic subunit. Fig. 5D and E demonstrate that expression of NRF2 and its targeted genes was substantially inhibited in HFD-fed ApoE$^{-/-}$LDLR$^{-/-}$ mouse heart. Treatment of the animals by high dose of simvastatin, CDDP or CDDP plus the low dose of simvastatin clearly restored their expression to normal levels. Similarly, *in vitro* OGD-increased cellular ROS levels were reduced by CDDP (Fig. 5F). OGD decreased expression of NRF2, SOD2 and CAT protein and mRNA, which were also potently reversed by CDDP in H9c2 and iPSC-CM cells (Fig. 5G and Fig. S7B).

Interestingly, treatment of H9c2 cells with PDCA induced NRF2 expression (Fig. S7C), indicating that KDM4A may also play an important role in CDDP-inhibited oxidative stress by regulating NRF2 pathway. Indeed, treatment of H9c2 cells with CDDP reversed OGD-induced KDM4A expression, which was associated with restoration of reduced NRF2, CAT and SOD2 expression (Fig. 5H). In addition, the co-treatment of CDDP and PDCA demonstrated greater effect on activation of NRF2, CAT and SOD2 expression and reduction of cellular ROS levels than either CDDP or PDCA alone since the co-treatment further inhibited KDM4A expression (Fig. 5H and I). Associated with changes of NRF2 expression, nuclear NRF2 levels were reduced by OGD while increased by PDCA, CDDP or CDDP plus PDCA with the greatest effect by CDDP plus PDCA (Fig. 5J), further confirming activation of NRF2 pathway by CDDP might be mediated through inactivation of KDM4A. Indeed, the similar results to PDCA were obtained when KDM4A expression was inhibited by KDM4A siRNA (si*KDM4A*) transfection (Fig. 5K). Furthermore, we determined that both DSDF and XST, the CDDP main components, also inhibited OGD-activated KDM4A expression to activate expression of NRF2, CAT and SOD2 and reduce OGD-induced cellular ROS levels (Fig. S7D–S7K), further confirming the role of KDM4A in CDDP-regulated NRF2 pathway.

NRF2 expression is negatively regulated by kelch-like ECH-associated protein 1 (KEAP1)[42]. *In vivo*, compared to WT mice, KEAP1 expression was increased in HFD-fed ApoE$^{-/-}$LDLR$^{-/-}$ mouse heart, which was reduced by high dose of simvastatin, CDDP and CDDP plus the low dose of simvastatin (Fig. S7L). *In vitro*, either CDDP or its components inhibited OGD-activated KEAP1 expression (Fig. S7M–S7O). These data suggest that anti-oxidative stress is another important anti-heart injury mechanism of CDDP with involvement of KDM4A-mediated NRF2 signaling pathway.

3.6. *CDDP blocks HFD-induced hepatic lipid accumulation and simvastatin-induced myolysis in skeletal muscle in HFD-fed ApoE$^{-/-}$LDLR$^{-/-}$ mice*

The long-term statin therapy or HFD feeding may cause some damages to tissues[43,44], which should be eliminated by CDDP in the case of co-treatment of CDDP and the low dose of simvastatin. Indeed, although CDDP had little effect on HFD-increased levels of serum alanine transaminase and total bile acid in ApoE$^{-/-}$LDLR$^{-/-}$ mice (Supporting Information Fig. S8A), HE or oil red O staining (Fig. S8B and Fig. 6A) and TG quantitative assay (Fig. 6B) show that CDDP or CDDP plus the low dose of simvastatin substantially attenuated HFD-induced lipid accumulation in the liver.

Consistently, increased serum TG levels in HFD-fed ApoE$^{-/-}$LDLR$^{-/-}$ mice were reduced by CDDP or CDDP plus the low dose of simvastatin (Fig. 6C), indicating anti-hypertriglyceridemia properties of CDDP. More importantly, the hypercholesterolemia in HFD-fed ApoE$^{-/-}$LDLR$^{-/-}$ mice was clearly reduced by CDDP or CDDP plus the low dose of simvastatin since serum cholesterol and low-density lipoprotein were reduced while high-density lipoprotein cholesterol increased (Fig. 6D), another important mechanism of CDDP reducing atherosclerosis and heart failure.

Mechanistically, expression of proteins for lipid synthesis, fatty acid synthase, stearoyl CoA desaturase 1, diacylglycerol *O*-acyltransferase, was reduced, while expression of proteins for lipid decomposition, hormone sensitive lipase and adipose triglyceride lipase, was activated by CDDP in HFD-fed ApoE$^{-/-}$LDLR$^{-/-}$ mouse liver (Fig. 6E). Interestingly, addition of the low dose of simvastatin to CDDP further enhanced the

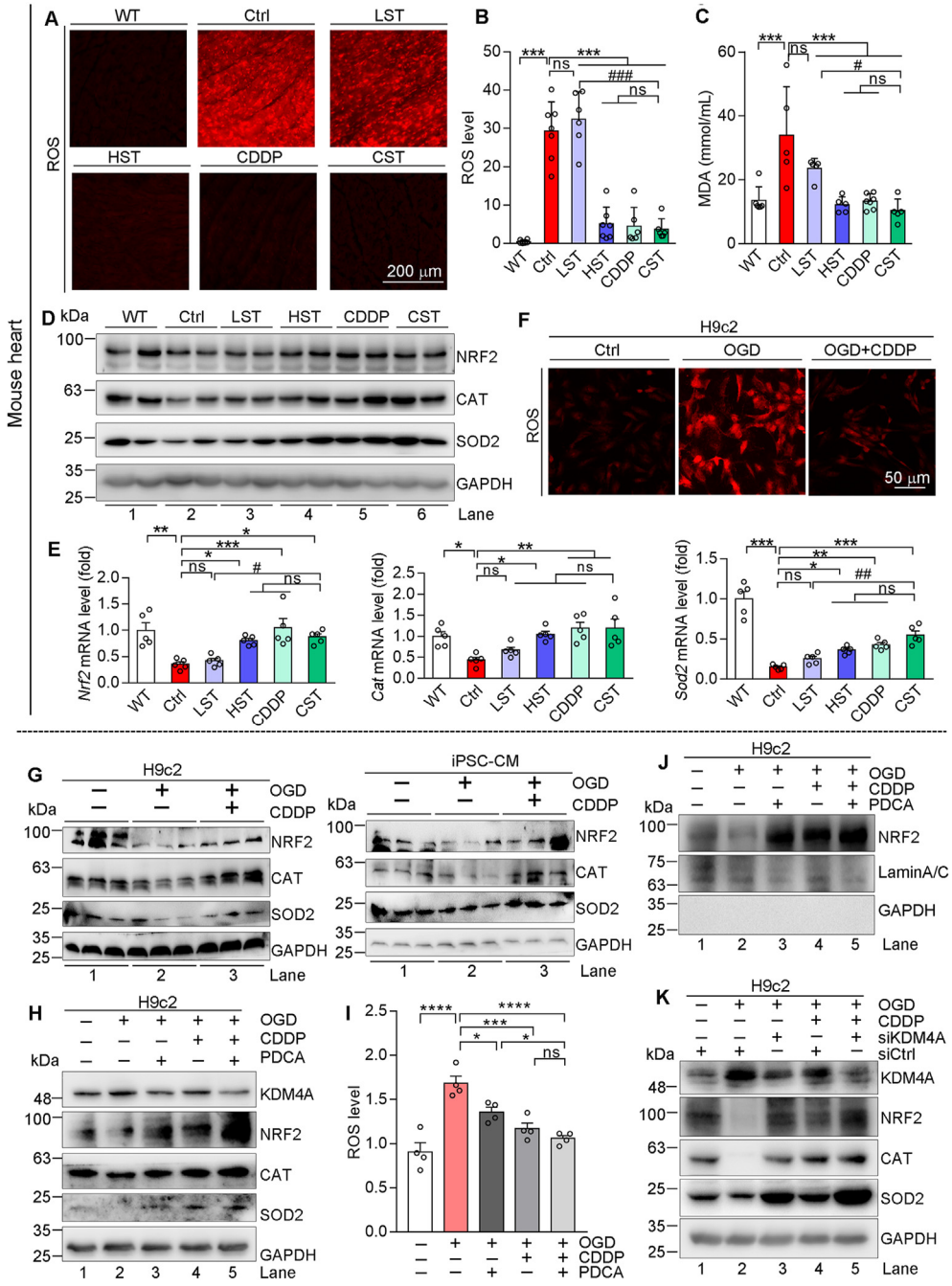

Figure 5 CDDP inhibits KDM4A to reduce oxidative stress. (A−E) Mouse heart samples in Fig. 1 were completed the following assays. ROS levels were determined by DHE staining of heart sections, and the images were photographed by a fluorescence microscope with quantification analysis of the fluorescent intensity (A, B, $n = 6$). MDA levels were determined by assay kit (C, $n = 5$). Protein expressions of NRF2, SOD2, CAT were determined by Western blot (D). Expression of *Nrf2*, *Sod2*, *Cat* mRNA was determined by qRT-PCR (E, $n = 5$). (F−K) H9c2 or iPSC-CM cells in OGD condition received the following treatment for 12 h, and the cells in normal culture condition were used as control: CDDP at 500 or 1000 μg/mL for H9c2 or iPSC-CM cells (F, G); CDDP at 500 μg/mL and/or PDCA at 1 μmol/L (H−J); cells were transfected with si*Ctrl* or si*KDM4A* as indicated, followed by CDDP (500 μg/mL) treatment (K). After treatment, cells were used to complete the following assays: cellular ROS levels by DHE staining (F) or ROS assay kit (I); expression NRF2, CAT, SOD2 and KDM4A in whole cellular extract (G, H, K) or NRF2 expression in nuclear extract (J) was determined by Western blot. The data are shown as mean ± SEM. $^{*}P < 0.05$, $^{**}P < 0.01$, $^{***}P < 0.001$; $^{\#}P < 0.05$, $^{\#\#\#}P < 0.001$; ns: not significantly different between indicated groups. MDA, malondialdehyde; ROS, reactive oxygen species; DHE, dihydroethidium.

effect of CDDP on expression of these molecules, particularly on lipid synthesis molecules (Fig. 6E). Activation of cholesterol 7α-hydroxylase (CYP7A1) and ATP binding cassette subfamily G member 5 (ABCG5) can enhance cholesterol catabolism in the liver. Reduction of ABCG5 and CYP7A1 expression in HFD-fed ApoE$^{-/-}$LDLR$^{-/-}$ mice suggests that in addition to increased cholesterol uptake from HFD, the reduced cholesterol catabolism can also make contributions to hypercholesterolemia. However,

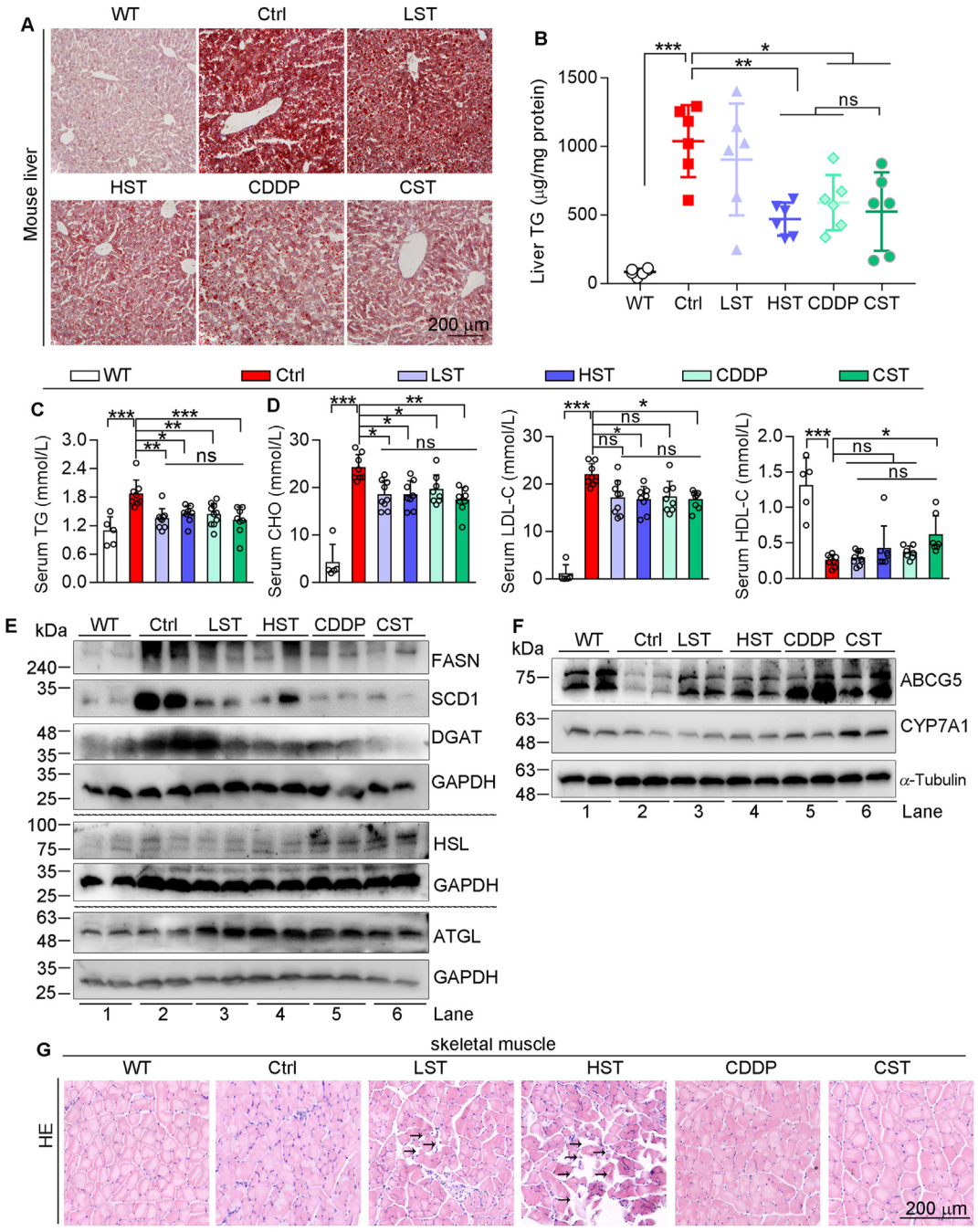

Figure 6 CDDP blocks HFD-induced hepatic lipid accumulation and simvastatin-induced myolysis in skeletal muscle. Serum and tissue samples of mice in Fig. 1 were conducted the following assays. Determination of hepatic lipid levels by oil red O staining of liver frozen sections (A) and TG quantitative assay (B). Levels of serum TG (C), CHO, LDL-C and HDL-C (D). The data are shown as mean ± SEM. $*P < 0.05$, $**P < 0.01$, $***P < 0.001$; ns: not significantly different between indicated gruops. Expression of FASN, SCD1, DGAT, HSL, ATGL (E), ABCG5 and CYP7A1 (F) protein in the liver was determined by Western blot. (G) HE staining of mouse skeletal muscle sections. ATGL, adipose triglyceride lipase; CHO, cholesterol; DGAT, diacylglycerol *O*-acyltransferase; FASN, fatty acid synthase; HDL-C, high-density lipoprotein cholesterol; HSL, hormone sensitive lipase; LDL-C, low-density lipoprotein cholesterol; SCD1, stearoyl CoA desaturase 1.

expression of ABCG5 and CYP7A1 was increased in mice received high dose of simvastatin, CDDP, or CDDP plus the low dose of simvastatin (Fig. 6F).

Statin therapy has been demonstrated some severe side effects, such as rhabdomyolysis[43]. Indeed, simvastatin caused myolysis in mouse skeletal muscle in a dose-dependent manner. CDDP alone had no effect on skeletal muscle structure. More importantly, CDDP blocked simvastatin-induced muscle injury (Fig. 6G), suggesting the high safety of CDDP in heart failure treatment.

4. Discussion

Heart failure is still the leading cause of death worldwide, which should be due to lack of the full understanding of its pathogenesis

and effective therapeutic strategies. Herein, we demonstrated that CDDP or CDDP combined a low dose of simvastatin can substantially reduce hypercholesterolemia/atherosclerosis-induced heart failure in ApoE$^{-/-}$LDLR$^{-/-}$ mice. In addition, CDDP blocked HFD-induced hepatic lipid accumulation and simvastatin-induced rhabdomyolysis, suggesting its potential application for heart failure treatment in clinic.

A few animal models have been generated for study the pathogenesis of heart failure and the development of therapeutic strategies, associated with obvious limitations. For instance, the heart failure generated by coronary artery ligation hardly happens to humans, while doxorubicin-caused heart failure can be observed only in some of cancer patients receiving chemotherapy[45]. In contrast, heart failure in many patients is caused by CHD[46], the disease associated with the long-term of hypercholesterolemia and atherosclerosis. Although hypercholesterolemia and atherosclerosis can be observed in LDLR or ApoE deficient mice, no report indicated they can develop heart failure. However, we speculated that in addition to hypercholesterolemia/atherosclerosis, the dual ApoE and LDLR deficiency in mice can generate additional risk factor(s) to cause heart dysfunctions. Indeed, after 16-week HFD feeding, in addition to hypercholesterolemia and advanced lesions (Figs. 1B and 6A−D, Fig. S2E), the typical features of heart failure were observed in ApoE$^{-/-}$LDLR$^{-/-}$ mice, such as decreased ejection fraction and fractional shortening, ST-segment depression in ECG and parameters for myocardial injury (Figs. 1D−F and 2). Pathologically, cardiac hypertrophy with myocardial structural disorder, infiltration of inflammatory cells, cardiac fibrosis and increased expression of heart failure markers were clearly observed in HFD-fed ApoE$^{-/-}$LDLR$^{-/-}$ mouse heart (Fig. 2). In contrast, we observed that mice with heterozygous LDLR and ApoE deficiency (ApoE$^{-/+}$LDLR$^{-/+}$) with 16-week HFD feeding or ApoE$^{-/-}$LDLR$^{-/-}$ mice with 8 weeks HFD feeding had normal heart functions, indicating the additional risk factor(s) brought by dual ApoE/LDLR deficiency plus the long-term hypercholesterolemia determine the occurrence of myocardia injury, which needs further investigation in the future. These results suggest that HFD-fed ApoE$^{-/-}$LDLR$^{-/-}$ mice might be a proper animal model which has close natural pathogenesis to heart failure in CHD patients. However, we did not detect coronary plaque and stenosis in the mice due to the technique limitations. Meanwhile, heart failure is the terminal stage of various heart diseases, and its clinical symptoms include dyspnea, ankle swelling and fatigue[47] are not easy to observe in mice. Therefore, more verifications should be completed to determine if this model is applicable for other kinds of heart failure.

Wnt pathway plays a key role in cardiac physiology and pathophysiology. Activation of Wnt pathway promotes cardiac regeneration processes and myocardial repair during cardiac injury[9,48]. However, the increasing evidence shows that aberrant Wnt pathway activation can lead to progression of onset cardiac dysfunction[49−52]. Thus, activated Wnt pathway is observed in patients or mice with heart failure. Reciprocally, inhibition of Wnt1/β-catenin, for instance by anti-miR-128, attenuates heart failure features in mice underwent transverse aortic constriction or treated with isoproterenol[53]. Consistently, by completing RNA-seq assay, we observed Wnt pathway was activated in HFD-fed ApoE$^{-/-}$LDLR$^{-/-}$ mouse heart, evidenced by reduced Wnt pathway inhibitor proteins and increased β-catenin. Associated with amelioration of heart failure, CDDP or CDDP plus the low dose of simvastatin resorted expression of Wnt pathway molecules to normal (Fig. 3). Similarly, CDDP reversed OGD-inhibited SFRP4/5, NKD1, BMP3, WIF1 and DKK2 expression and OGD-activated β-catenin expression in H9c2 cardiomyocytes (Fig. S4C and S4E). In contrast, OGD inhibited while CDDP activated β-catenin expression in iPSC-CM cells (Fig. S4D). The opposite results of β-catenin by OGD might be due to the different effects of OGD on cell death between H9c2 and iPSC-CM cells. In fact, iPSC-CM cells, but not H9c2 cells, underwent death by OGD treatment, which may decrease β-catenin expression, while CDDP protected cells against OGD-induced cell death to enhance cell survival by partial recovering decreased β-catenin expression. In addition, the anti-Wnt pathway by CDDP in iPSC-CM cells might be completed through inactivation of non-canonical Wnt pathway, which is independent of β-catenin expression, based on the fact that SFRP4/5, WIF1, NKD1 and DKK2 can also participate in non-canonical Wnt pathway[7,54,55]. Therefore, we believe that CDDP demonstrates dual regulatory effect on Wnt pathway that it protects iPSC-CM cells against OGD-induced damage through inactivation of the non-canonical Wnt pathway while enhancing cell viability by activating canonical Wnt pathway. The dual regulation of Wnt pathway by CDDP might be in cell type-dependent manner, which needs more investigation in the future. Taken together, our study not only confirms the pathogenic role of Wnt pathway, but also identifies an important mechanism for anti-heart failure by CDDP.

In this study, we demonstrated that KDM4A is involved in CDDP-inhibited inflammation. The previous studies indicated KDM4A is positively correlated to inflammation levels in ischemic stroke[15], and involved in transverse aortic constriction surgery-caused myocardial hypertrophy in mice[17]. We initially observed that CDDP reduced infiltration of inflammatory cells into HFD-fed ApoE$^{-/-}$LDLR$^{-/-}$ mouse heart (Fig. 2J), associated with reduction of HFD-increased levels of IL-1β and TNF-α in mouse serum, and expression of P65, p-P65, IL-1β and TNF-α in mouse heart or OGD-treated cardiomyocytes (Fig. 4A, B and G−J; Fig. S5A). We then detected that the anti-inflammation by CDDP is clearly related to inhibition of KDM4 activity and expression by determining the high binding affinity of CDDP/component to KDM4A (Fig. 4D−F) and the reduction of KDM4A protein expression in either mouse heart or cardiomyocytes (Fig. 4B and G) by CDDP. Treatments of CDDP or its main component (DSDF and XST) to RAW 264.7 macrophages (the main cell type with occurrence of inflammation) also reduced expression of total and phosphorylated P65, associated with inhibition of expression and secretion and IL-1β and TNF-α (Fig. 4H and I; Fig. S5I, S5J, S5L and S5M). We further determined the anti-inflammation by CDDP or its components is associated with inhibition of KDM4A expression (Fig. 4H−J; Fig. S5I−S5N) in RAW 264.7 macrophages. However, the anti-inflammation effect by CDDP or its component plus PDCA/si*KDM4A* was similar to that by PDCA/si*KDM4A* alone, indicating CDDP may mainly repress inflammation *via* KDM4A pathway in macrophages. Considering the main biological function of KDM4[56], we determined that CDDP increased methylation of *P65* promoter and inhibited P65 expression in mouse heart (Fig. S6C, Fig. 4B), suggesting the anti-inflammation by CDDP should be attributed to activation of *P65* promoter methylation.

It has been shown that JMJD3 (KDM6B), a member of the histone demethylase family, decreased H3K27me3 enrichment on *β-Mhc* promoter region, and subsequently increased β-MHC expression, thereby contributing to isoproterenol-induced cardiac hypertrophy[57]. In our study, we observed that CDDP reduced HFD-activated *β-Mhc* mRNA expression in ApoE$^{-/-}$LDLR$^{-/-}$ mouse heart (Fig. 2I), associated with increased methylation of *β-Mhc* promoter (Fig. S6D), which should also be attributed to CDDP-inhibited KDM4A.

CDDP has been reported to inhibit ROS production to protect heart injury[18] with unclear involved mechanisms. Associated with inhibition of KDM4A expression, CDDP reversed inhibition of

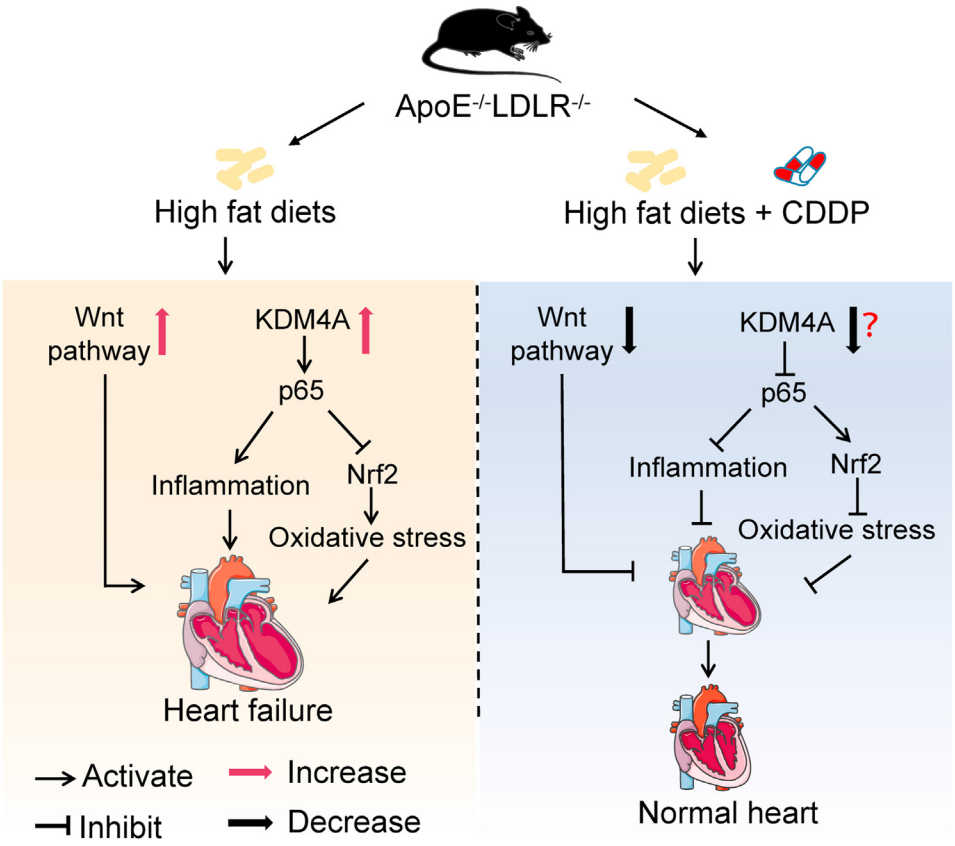

Figure 7 The diagram illustrates the mechanisms by which CDDP protects ApoE$^{-/-}$LDLR$^{-/-}$ mice against hypercholesterolemia/atherosclerosis-induced heart failure. The long-term high-fat diet feeding induces hypercholesterolemia and atherosclerosis in ApoE$^{-/-}$LDLR$^{-/-}$ mice, which results in activation of KDM4A. The activated KDM4A in cardiomyocytes induces inflammation and oxidative stress to facilitate heart injury. However, treatment of the mice with CDDP may potently reduce KDM4A expression and activity. Combined inhibition on Wnt pathway, CDDP effectively ameliorates heart failure.

NRF2 expression in ApoE$^{-/-}$LDLR$^{-/-}$ mouse heart (Fig. 5D and E). In addition, PDCA, a KDM4A chemical inhibitor, also activated NRF2 expression/activity, which was further enhanced by CDDP or its components in cardiomyocytes (Fig. 5I, J, Fig. S7D and S7H) which might be due to the more inhibition of KDM4A expression by the co-treatment. Meanwhile, the similar results were obtained when KDM4A expression was inhibited by siRNA (Fig. 5K; Fig. S7G and S7K). In addition, expression of KEAP1, the negative regulator of NRF2 was inhibited by PDCA, CDDP or its components (Fig. S7C, S7L–S7O), further suggesting activation of NRF2 pathway by CDDP is related to inhibition of KDM4A expression. Interestingly, the inaction between NF-κB p65 and NRF2 can mutual regulate activity of each other[58,59]. Thus, although no changes of *Nrf2* promoter methylation were observed, the activation of NRF2 pathway by CDDP can be partially attributed to inactivation of NF-κB through increased *P*65 methylation. Taken together, our study demonstrates that regulation of KDM4 activity plays a critical role in CDDP-inhibited inflammation and oxidative stress. However, currently we do not have direct evidence that KDM4A plays a causal role in the protective effects of CDDP against hypercholesterolemia/atherosclerosis induced heart failure in mice. Future studies are needed to use KDM4A knockout mice to further dissect the role of KDM4A in the protective effects of CDDP in heart failure.

In addition to anti-hypercholesterolemia/atherosclerosis, statins also stabilize/reduce myocardial infarction[60]. However, the long-term statin therapy may cause muscle damage[4]. Indeed, simvastatin reduced atherosclerosis and myocardial injury while caused rhabdomyolysis in a dose-dependent manner in HFD-fed ApoE$^{-/-}$LDLR$^{-/-}$ mice (Figs. 1, 2 and 6; Fig. S2E). Surprisingly, CDDP demonstrated comparable anti-hypercholesterolemia/atherosclerosis and heart injury functions to that by the high dose of simvastatin which clearly exceeds the recommended dose in clinic. More importantly, CDDP substantially blocked simvastatin-caused muscle damage (Fig. 6G).

Although CDDP demonstrated comparable anti-hypercholesterolemic effects to the low dose of simvastatin (Fig. 6D), it had more potent inhibitory effects on atherosclerosis and myocardial injury (Figs. 1B, C and 2; Fig. S2E), implying that CDDP may have additional mechanisms to reduce atherosclerosis and heart injury. Interestingly, addition of CDDP to the low dose of simvastatin demonstrated better inhibitory effects on atherosclerosis and heart failure than simvastatin alone. In addition, the combination can further ameliorate lipid profiles (Fig. 6A–E), which is consistent with the observations in clinic (Supporting Information Fig. S9). The results of meta-analysis also show that combined CDDP and statins significantly reduces left ventricular end diastolic diameter and left ventricular ejection fraction in CHD patients

(Fig. S3D and S3E), thereby ameliorating cardiac systolic function and cardiovascular disease. Taken together, these studies demonstrate the importance of combined CDDP and low dose of statin in CHD treatment in clinic.

5. Conclusions

Our study demonstrates that associated with hypercholesterolemia/atherosclerosis, HFD-fed ApoE$^{-/-}$LDLR$^{-/-}$ mice can develop severe heart injury. CDDP not only protects mice against heart failure, but also blocks simvastatin-induced rhabdomyolysis. Mechanistically, the anti-heart injury properties of CDDP should be attributed to inactivation of Wnt pathway, anti-inflammation and anti-oxidative stress with involvement of regulation of KDM4 expression/activity (Fig. 7). Our study suggests that CDDP or combined a low dose of simvastatin can be an effective therapy for treatment of hypercholesterolemia/atherosclerosis-induced heart failure.

Acknowledgments

This study was supported by the China NSFC grants 82173807 to Yajun Duan and 81973316 to Jihong Han; Tianjin Municipal Science and Technology Commission of China Grant 20JCZDJC00710 and the Fundamental Research Funds for the Central Universities (Nankai University, China) 63211045 to Jihong Han.

On January 21, 2023, Professor Jihong Han passed away in Hefei, Anhui province, China. He is a pharmacologist in the field of basic and translational research of atherosclerosis, 'Yangtze River scholars' Distinguished Professor of Chinese Ministry of Education, chief scientist of the National Basic Research Program of China (973 Program) held by Chinese Ministry of Science and Technology. All the other authors are honored to have accomplished this study along with Professor Jihong Han, deeply miss and pay tribute to him.

Author contributions

Yanfang Yang, Ke Feng, Yajun Duan, Jihong Han and Yunhui Hu designed the study, drafted and edited the manuscript; Yanfang Yang, Ke Feng, Liying Yuan and Yuxin Liu performed most of the experiments; Mengying Zhang, Kaimin Guo, Zequn Yin, Wenjia Wang, Shuiping Zhou, He Sun, Kaijing Yan, Xijun Yan and Xuerui Wang assisted with the experimental operation or data collection.

Conflicts of interest

Authors MZ, KG, WW and YH are employee of GeneNet Pharmaceuticals Co., Ltd. Authors SZ and XY are employee of Tasly Pharmaceutical Group Co., Ltd. Authors KY and HS are employee of GeneNet Pharmaceuticals Co., Ltd. and Tasly Pharmaceutical Group Co., Ltd. The rest authors declare have no conflict of interest with this work.

Appendix A. Supporting information

Supporting data to this article can be found online at https://doi.org/10.1016/j.apsb.2022.11.012.

References

1. Tanai E, Frantz S. Pathophysiology of heart failure. *Compr Physiol* 2016;**6**:187−214.
2. He Y, Huang W, Zhang C, Chen L, Xu R, Li N, et al. Energy metabolism disorders and potential therapeutic drugs in heart failure. *Acta Pharm Sin B* 2021;**11**:1098−116.
3. Rush CJ, Campbell RT, Jhund PS, Petrie MC, McMurray JJV. Association is not causation: treatment effects cannot be estimated from observational data in heart failure. *Eur Heart J* 2018;**39**:3417−38.
4. Tomaszewski M, Stepien KM, Tomaszewska J, Czuczwar SJ. Statin-induced myopathies. *Pharmacol Rep* 2011;**63**:859−66.
5. Luo J, Song W, Yang G, Xu H, Chen K. Compound Danshen (*Salvia miltiorrhiza*) dripping pill for coronary heart disease: an overview of systematic reviews. *Am J Chin Med* 2015;**43**:25−43.
6. Zhou W, Yuan WF, Chen C, Wang SM, Liang SW. Study on material base and action mechanism of compound Danshen dripping pills for treatment of atherosclerosis based on modularity analysis. *J Ethnopharmacol* 2016;**193**:36−44.
7. Nusse R, Clevers H. Wnt/beta-catenin signaling, disease, and emerging therapeutic modalities. *Cell* 2017;**169**:985−99.
8. Foulquier S, Daskalopoulos EP, Lluri G, Hermans KCM, Deb A, Blankesteijn WM. WNT signaling in cardiac and vascular disease. *Pharmacol Rev* 2018;**70**:68−141.
9. Liu S, Tang L, Zhao X, Nguyen B, Heallen TR, Li M, et al. Yap promotes noncanonical Wnt signals from cardiomyocytes for heart regeneration. *Circ Res* 2021;**129**:782−97.
10. Xiang FL, Fang M, Yutzey KE. Loss of beta-catenin in resident cardiac fibroblasts attenuates fibrosis induced by pressure overload in mice. *Nat Commun* 2017;**8**:712.
11. Hou N, Ye B, Li X, Margulies KB, Xu H, Wang X, et al. Transcription factor 7-like 2 mediates canonical Wnt/beta-catenin signaling and c-Myc upregulation in heart failure. *Circ Heart Fail* 2016;**9**:10.1161/CIRCHEARTFAILURE.116.003010 e003010.
12. Young NL, Dere R. Mechanistic insights into KDM4A driven genomic instability. *Biochem Soc Trans* 2021;**49**:93−105.
13. Labbe RM, Holowatyj A, Yang ZQ. Histone lysine demethylase (KDM) subfamily 4: structures, functions and therapeutic potential. *Am J Transl Res* 2014;**6**:1−15.
14. Lee DH, Kim GW, Jeon YH, Yoo J, Lee SW, Kwon SH. Advances in histone demethylase KDM4 as cancer therapeutic targets. *FASEB J* 2020;**34**:3461−84.
15. Liu Y, Zhao L, Zhang J, Lv L, Han K, Huang C, et al. Histone demethylase KDM4A inhibition represses neuroinflammation and improves functional recovery in ischemic stroke. *Curr Pharmaceut Des* 2021;**27**:2528−36.
16. Zhang YY, Yuan YB, Li ZL, Chen H, Fang MM, Xiao PX, et al. An interaction between BRG1 and histone modifying enzymes mediates lipopolysaccharide-induced proinflammatory cytokines in vascular endothelial cells. *J Cell Biochem* 2019;**120**:13216−25.
17. Zhang QJ, Chen HZ, Wang L, Liu DP, Hill JA, Liu ZP. The histone trimethyllysine demethylase JMJD2A promotes cardiac hypertrophy in response to hypertrophic stimuli in mice. *J Clin Invest* 2011;**121**:2447−56.
18. Feng K, Liu Y, Sun J, Zhao C, Duan Y, Wang W, et al. Compound Danshen dripping pill inhibits doxorubicin or isoproterenol-induced cardiotoxicity. *Biomed Pharmacother* 2021;**138**:111531.
19. Huang DW, Sherman BT, Lempicki RA. Systematic and integrative analysis of large gene lists using DAVID bioinformatics resources. *Nat Protoc* 2009;**4**:44−57.
20. Choi M, Lee J, Le MT, Nguyen DT, Park S, Soundrarajan N, et al. Genome-wide analysis of DNA methylation in pigs using reduced representation bisulfite sequencing. *DNA Res* 2015;**22**:343−55.
21. Pinero J, Bravo A, Queralt-Rosinach N, Gutierrez-Sacristan A, Deu-Pons J, Centeno E, et al. DisGeNET: a comprehensive platform integrating information on human disease-associated genes and variants. *Nucleic Acids Res* 2017;**45**:D833−9.

22. Wishart DS, Feunang YD, Guo AC, Lo EJ, Marcu A, Grant JR, et al. DrugBank 5.0: a major update to the DrugBank database for 2018. *Nucleic Acids Res* 2018;**46**:D1074−82.
23. Wang YL, Bryant SH, Cheng TJ, Wang JY, Gindulyte A, Shoemaker BA, et al. PubChem BioAssay: 2017 update. *Nucleic Acids Res* 2017;**45**:D955−63.
24. Zhang S, Guo FL, Yu M, Yang XX, Yao Z, Li Q, et al. Reduced Nogo expression inhibits diet-induced metabolic disorders by regulating ChREBP and insulin activity. *J Hepatol* 2020;**73**:1482−95.
25. Nie Z, Shi LH, Lai C, O'Connell SM, Xu JC, Stansfield RK, et al. Structure-based design and discovery of potent and selective KDM5 inhibitors. *Bioorg Med Chem Lett* 2018;**28**:1490−4.
26. Liu P, Yang H, Long F, Hao HP, Xu XJ, Liu Y, et al. Bioactive equivalence of combinatorial components identified in screening of an herbal medicine. *Pharm Res* 2014;**31**:1788−800.
27. Li W, Zhou H, Chu Y, Wang X, Luo R, Yang L, et al. Simultaneous determination and pharmacokinetics of danshensu, protocatechuic aldehyde, 4-hydroxy-3-methyloxyphenyl lactic acid and protocatechuic acid in human plasma by LC−MS/MS after oral administration of compound Danshen dripping pills. *J Pharm Biomed Anal* 2017;**145**:860−4.
28. Gao S, Han L, Luo D, Liu G, Xiao Z, Shan G, et al. Modeling drug mechanism of action with large scale gene-expression profiles using GPAR, an artificial intelligence platform. *BMC Bioinf* 2021;**22**:17.
29. Redfield MM. Heart failure—an epidemic of uncertain proportions. *N Engl J Med* 2002;**347**:1442−4.
30. Liao J, Huang W, Liu G. Animal models of coronary heart disease. *J Biomed Res* 2015;**30**:3−10.
31. Tang YP, Liu Y, Fan YJ, Zhao YY, Feng JQ, Liu Y. To develop a novel animal model of myocardial infarction: a research imperative. *Animal Model Exp Med* 2018;**1**:36−9.
32. Sassi Y, Avramopoulos P, Ramanujam D, Grueter L, Werfel S, Giosele S, et al. Cardiac myocyte miR-29 promotes pathological remodeling of the heart by activating Wnt signaling. *Nat Commun* 2017;**8**:1614.
33. Malekar P, Hagenmueller M, Anyanwu A, Buss S, Streit MR, Weiss CS, et al. Wnt signaling is critical for maladaptive cardiac hypertrophy and accelerates myocardial remodeling. *Hypertension* 2010;**55**:939−45.
34. Travers JG, Kamal FA, Valiente-Alandi I, Nieman ML, Sargent MA, Lorenz JN, et al. Pharmacological and activated fibroblast targeting of G beta gamma-GRK2 after myocardial ischemia attenuates heart failure progression. *J Am Coll Cardiol* 2017;**70**:958−71.
35. Marti-Pamies I, Thoonen R, Seale P, Vite A, Caplan A, Tamez J, et al. Deficiency of bone morphogenetic protein-3b induces metabolic syndrome and increases adipogenesis. *Am J Physiol Endocrinol Metab* 2020;**319**:E363−75.
36. Hino J, Matsuo H, Kangawa K. Bone morphogenetic protein-3b (*BMP-3b*) gene expression is correlated with differentiation in rat calvarial osteoblasts. *Biochem Biophys Res Commun* 1999;**256**:419−24.
37. Qi D, Atsina K, Qu L, Hu X, Wu X, Xu B, et al. The vestigial enzyme D-dopachrome tautomerase protects the heart against ischemic injury. *J Clin Invest* 2014;**124**:3540−50.
38. Verma SK, Krishnamurthy P, Barefield D, Singh N, Gupta R, Lambers E, et al. Interleukin-10 treatment attenuates pressure overload-induced hypertrophic remodeling and improves heart function *via* signal transducers and activators of transcription 3-dependent inhibition of nuclear factor-kappa B. *Circulation* 2012;**126**:418−29.
39. Young LC, Hendzel MJ. The oncogenic potential of Jumonji D2 (JMJD2/KDM4) histone demethylase overexpression. *Biochem Cell Biol* 2013;**91**:369−77.
40. Muenzel T, Gori T, Keaney Jr JF, Maack C, Daiber A. Pathophysiological role of oxidative stress in systolic and diastolic heart failure and its therapeutic implications. *Eur Heart J* 2015;**36**:2555−64.
41. Hu C, Zhang X, Wei W, Zhang N, Wu H, Ma Z, et al. Matrine attenuates oxidative stress and cardiomyocyte apoptosis in doxorubicin-induced cardiotoxicity *via* maintaining AMPKalpha/UCP2 pathway. *Acta Pharm Sin B* 2019;**9**:690−701.
42. Bellezza I, Giambanco I, Minelli A, Donato R. Nrf2−Keap1 signaling in oxidative and reductive stress. *Biochim Biophys Acta Mol Cell Res* 2018;**1865**:721−33.
43. Thompson PD, Panza G, Zaleski A, Taylor B. Statin-associated aide effects. *J Am Coll Cardiol* 2016;**67**:2395−410.
44. Malesza IJ, Malesza M, Walkowiak J, Mussin N, Walkowiak D, Aringazina R, et al. High-fat, western-style diet, systemic inflammation, and gut microbiota: a narrative review. *Cells* 2021;**10**:3164.
45. Carvalho C, Santos RX, Cardoso S, Correia S, Oliveira PJ, Santos MS, et al. Doxorubicin: the good, the bad and the ugly effect. *Curr Med Chem* 2009;**16**:3267−85.
46. Morbach C, Wagner M, Guntner S, Malsch C, Oezkur M, Wood D, et al. Heart failure in patients with coronary heart disease: prevalence, characteristics and guideline implementation—results from the German EuroAspire IV cohort. *BMC Cardiovasc Disord* 2017;**17**:108.
47. Chaudhry SI, Wang YF, Concato J, Gill TM, Krumholz HM. Patterns of weight change preceding hospitalization for heart failure. *Circulation* 2007;**116**:1549−54.
48. Duan JZ, Gherghe C, Liu DX, Hamlett E, Srikantha L, Rodgers L, et al. Wnt1/beta catenin injury response activates the epicardium and cardiac fibroblasts to promote cardiac repair. *EMBO J* 2012;**31**:429−42.
49. Goto J, Otaki Y, Watanabe T, Kobayashi Y, Aono T, Watanabe K, et al. HECT (homologous to the E6-AP carboxyl terminus)-type ubiquitin E3 ligase ITCH attenuates cardiac hypertrophy by suppressing the Wnt/beta-catenin signaling pathway. *Hypertension* 2020;**76**:1868−78.
50. Li ZK, Zhu SX, Liu Q, Wei JL, Jin YC, Wang XF, et al. Polystyrene microplastics cause cardiac fibrosis by activating Wnt/beta-catenin signaling pathway and promoting cardiomyocyte apoptosis in rats. *Environ Pollut* 2020;**265**:115025.
51. Dawson K, Aflaki M, Nattel S. Role of the Wnt-Frizzled system in cardiac pathophysiology: a rapidly developing, poorly understood area with enormous potential. *J Physiol* 2013;**591**:1409−32.
52. Fu WB, Wang WE, Zeng CY. Wnt signaling pathways in myocardial infarction and the therapeutic effects of Wnt pathway inhibitors. *Acta Pharmacol Sin* 2019;**40**:9−12.
53. Li JY, Li XC, Tang YL. Upregulation of miR-128 mediates heart injury by activating Wnt/beta-catenin signaling pathway in heart failure mice. *Organogenesis* 2021;**17**:27−39.
54. Meyer IS, Jungmann A, Dieterich C, Zhang M, Lasitschka F, Werkmeister S, et al. The cardiac microenvironment uses non-canonical WNT signaling to activate monocytes after myocardial infarction. *EMBO Mol Med* 2017;**9**:1279−93.
55. Van Raay TJ, Coffey RJ, Soinica-Krezel L. Zebrafish naked1 and naked2 antagonize both canonical and non-canonical Wnt signaling. *Dev Biol* 2007;**309**:151−68.
56. Black JC, Van Rechem C, Whetstine JR. Histone lysine methylation dynamics: establishment, regulation, and biological impact. *Mol Cell* 2012;**48**:491−507.
57. Guo Z, Lu J, Li JY, Wang PX, Li ZZ, Zhong Y, et al. JMJD3 inhibition protects against isoproterenol-induced cardiac hypertrophy by suppressing beta-MHC expression. *Mol Cell Endocrinol* 2018;**477**:1−14.
58. Wardyn JD, Ponsford AH, Sanderson CM. Dissecting molecular cross-talk between Nrf2 and NF-kappa B response pathways. *Biochem Soc Trans* 2015;**43**:621−6.
59. Hu B, Wei HJ, Song YH, Chen MM, Fan ZY, Qiu RL, et al. NF-kappa B and Keap1 interaction represses Nrf2-mediated antioxidant response in rabbit hemorrhagic disease virus infection. *J Virol* 2020;**94**:e00016−20.
60. Arnold SV, Kosiborod M, Tang FM, Zhao ZX, Maddox TM, McCollam PL, et al. Patterns of statin initiation, intensification, and maximization among patients hospitalized with an acute myocardial infarction. *Circulation* 2014;**129**:1303−9.